

Self-consistency and continuity questions on axisymmetric, rigidly rotating polytropes

R. Caimmi*

October 11, 2018

Abstract

Axisymmetric, rigidly rotating polytropes are considered in the framework of both the original Chandrasekhar (C33) approximation and a different version (extended C33 approximation). Special effort is devoted to two specific points, namely (i) a contradiction between the binomial series evaluation, $(\theta_w + \Delta\theta)^n \approx \theta_w^n + n\theta_w^{n-1}\Delta\theta$, implying $|\Delta\theta| \ll |\theta_w|$, and the vanishing density on the boundary, implying $\theta_w \rightarrow 0$, which affects the self-consistency of the above mentioned approximations, and (ii) the continuity of selected parameters as a function of the polytropic index, n . Concerning (i), it is shown Emden-Chandrasekhar (EC) associated functions, θ_0 , θ_2 , and ψ_0 , ψ_2 , are defined at any internal point even if related EC associated equations hold only for a particular subvolume, in the framework of the extended C33 and the C33 approximation, respectively. Concerning (ii), the continuity may safely be established in the limit, $n \rightarrow 0$, $n \rightarrow 5$, for part of the parameters, while additional data are needed for the remaining part. Simple fitting curves, valid to a good extent for a wide range of n , involve exponential functions and, in a single case, two straight lines joined by a parabolic segment. The expression of physical parameters in terms of the polytropic index can be used in building up sequences of configurations with changing density profile for assigned mass and angular momentum.

**Physics and Astronomy Department, Padua University, Vicolo Osservatorio 3/2, I-35122 Padova, Italy* email: roberto.caimmi@unipd.it fax: 39-049-8278212

*keywords - stars: equilibrium - galaxies: equilibrium - polytropes:
rigid rotation.*

1 Introduction

A main part of astrophysical bodies, such as stars, galaxies, clusters of galaxies, are characterized by the occurrence of three kinds of forces, due to gravitation, rotation and pressure or stress tensor. Density profiles are, in principle, lying between the extreme cases of homogeneous (constant density) and Roche (mass point surrounded by a vanishing atmosphere) equilibrium configurations, respectively. A simple description implies strong restrictions, such as homogeneity, spherical symmetry, rigid rotation.

The effect of rigid rotation on homogeneous (incompressible) ellipsoids has been studied since a long time (e.g., MacLaurin 1742; Jacobi 1834; Dedekind 1860; Riemann 1860; Jeans 1929, Chap. VIII). For further details, exhaustive presentation and complete references, an interested reader is addressed to specific textbooks (e.g., Chandrasekhar 1969).

The effect of different density profiles on nonrotating (spherical) polytropes has also been studied since a long time (e.g., Lane 1870; Ritter 1878; Schuster 1883; Thomson 1887; Emden 1907; Chandrasekhar 1939, Chap. IV). For further details, exhaustive presentation and complete references, an interested reader is addressed to specific textbooks (e.g., Horedt 2004).

On the other hand, less effort has been devoted to the combined effect of different rotation and density profiles on polytropes, due to a larger complexity of the problem and the absence of electronic computers in the past. When a critical rotation is attained, two different kinds of instability can occur, namely (i) centrifugal breakup via shedding of matter on the equatorial plane, for sufficiently steep density profiles, and (ii) fissional breakup after transition from axisymmetric to triaxial configurations, for sufficiently mild density profiles. Shedding of matter occurs via rings or opposite streams according if related configurations are axisymmetric or triaxial, respectively. For further details, exhaustive presentation and complete references, an interested reader is addressed to specific textbooks (e.g., Jeans 1929, Chap. IX).

A simple and elegant first-order approximation, which implies small departure from spherical shape, makes physical quantities depend on a rotation parameter, $v = \Omega^2/(2\pi G\lambda)$, where Ω is the angular velocity, G the constant of gravitation, λ the central density. Related systems shall be quoted in the following as Emden-Chandrasekhar, axisymmetric, rigidly rotating polytropes or, in short, EC polytropes. For further details, exhaustive presentation and complete references, an interested reader is addressed to the parent paper

(Chandrasekhar 1933a, hereafter quoted as C33), and later investigations, (Chandrasekhar 1933b; Chandrasekhar and Lebovitz 1962).

Unfortunately, the correction terms are inferred from differential equations (hereafter quoted as EC associated equations) where the zero-th order term is divergent on the boundary for sufficiently mild density profiles, concerning polytropic index within the range, $0 \leq n < 1$. It is worth remembering that homogeneous and extended Roche (maximal concentration: finite mass extending up to infinity or mass point surrounded by a vanishing atmosphere within a finite region) configurations relate to $n = 0$ and $n = 5$, respectively. The above mentioned correction terms involve Legendre polynomials of degree 0 and 2, $P_0(\mu)$ and $P_2(\mu)$, respectively.

With regard to radial distortions, related to $P_0(\mu)$, the correction term, χ_0 , may be incorporated into the unperturbed radial function, θ_E , and the resulting perturbed radial function, $\theta_0(\xi, v) = \theta_E(\xi) + \chi_0(\xi, v)$, is the solution of a generalized Lane-Emden equation where rotation is also included. Accordingly, the above mentioned inconvenient is avoided at the price that the correction terms, χ_0 , $A_2\theta_2$, depend on the rotation parameter, v , contrary to their counterparts in C33 approximation, $v\psi_0$, $vC_2\psi_2$, where the rotation parameter appears as a factor. In the nonrotating limit, $v \rightarrow 0$, the following relations hold:

$$\lim_{v \rightarrow 0} \frac{\chi_0(\xi, v)}{v} = \psi_0(\xi) \quad ; \quad \lim_{v \rightarrow 0} \frac{A_2(v)\theta_2(\xi, v)}{C_2v} = \psi_2(\xi) \quad ; \quad (1)$$

where, keeping in mind both $\theta_2(\xi, v)$ and $\psi_2(\xi)$ are undetermined by a multiplicative constant, the relation on the right-hand side can be splitted as:

$$\lim_{v \rightarrow 0} \frac{A_2(v)}{v} = C_2 \quad ; \quad \lim_{v \rightarrow 0} \theta_2(\xi, v) = \psi_2(\xi) \quad ; \quad (2)$$

as shown below in dealing with the general theory.

The approximation under discussion shall be quoted in the following as the extended C33 approximation. Related systems shall be quoted as EC polytropes, similarly to their counterparts within the framework of the C33 approximation. For further details, exhaustive presentation and additional references, an interested reader is addressed to earlier attempts (Caimmi 1980, 1983, 1985, 1987, 1988; hereafter quoted as C80, C83, C85, C87, C88, respectively).

With regard to both radial and meridional (i.e. depending on the polar angle) distortion, the EC associated equations are formulated by use of the power-series approximation, $\theta^n = (\theta_w + \Delta\theta)^n \approx \theta_w^n + n\theta_w^{n-1}\Delta\theta$ which implies (C33; C83):

$$\left| \frac{\Delta\theta}{\theta_w} \right| \ll 1 \quad ; \quad w = E, 0 \quad ; \quad (3)$$

where θ^n is the distorted dimensionless density, θ_w^n its undistorted or radially distorted counterpart, according if $w = E$ (C33 approximation) or $w = 0$ (extended C33 approximation), respectively, $\Delta\theta$ is the global or meridional distortion term, and $|\Delta\theta/\theta_w|$ may be considered as a distortion index. For further details, exhaustive presentation and complete references, an interested reader is addressed to the parent papers (C33; C83).

The above inequality is clearly satisfied in the central region of the system, where $\theta_w \lesssim 1$ and distortion due to rigid rotation is small. Conversely, the requisite of vanishing density on the boundary of the undistorted or radially distorted sphere, $\theta_w(\Xi_w) = 0$, makes Eq. (3) violated, keeping in mind distortion due to rigid rotation is maximum on the boundary. Accordingly, Eq. (3) is expected to hold above a threshold, $\theta_w > \epsilon_w^*$, where ϵ_w^* depends on an assumed tolerance, 10% say.

The equilibrium equation of EC polytropes (hereafter quoted as EC equation), together with the EC associated equations, have analytic solutions only in the special cases, $n = 0, 1, 5$, (e.g., C33; Chandrasekhar 1939, Chap. IV; C80; C87; Horedt 1990, hereafter quoted as H90; Horedt 2004, Chap. 2). The comparison of related physical parameters with their counterparts, numerically computed in a close neighbourhood of the above mentioned values of n , may be a useful test for establishing the dependence on the polytropic index.

For instance, a monotonic trend is shown by Ξ_E , $\theta'_E(\Xi_E)$, contrary to $\theta''_E(\Xi_E)$ and EC associated functions together with their first and second derivatives. More specifically, the first derivatives of the EC associated functions could be monotonic in absence of continuity at $n = 0$, according to H90 results, while the contrary holds in presence of continuity, according to C83 results, plotted¹ therein and listed in a later attempt (C85). The second derivative, $\psi''_2(\Xi_E)$, is divergent within the range, $0 < n < 1$. In conclusion, further investigation should be needed about the continuity of physical parameters related to EC polytropes in the limit, $n \rightarrow 0$, within the framework of C33 approximation.

Concerning the opposite limit, $n \rightarrow 5$, it has been noticed that, in the nonrotating case, the dimensionless mass as a function of n exhibits a slight nonmonotonic trend with a minimum within the range, $4.80 < n < 4.85$, (Seidov and Kuzakhmedov 1978). A similar result holds for rigidly rotating configurations (C85) which implies a slight nonmonotonic trend with a maximum, within the above mentioned range, for the axis ratio at the onset of equatorial breakup (C87). Further investigation to this respect should be needed on other physical parameters, and the continuity in the limit, $n \rightarrow 5$,

¹ With regard to Fig. 1 therein and related caption, θ'_0 has erroneously been written instead of θ''_0 and vice versa.

should also be tested within the framework of C33 approximation.

Polytropes span over the whole range of configurations with regard not only to density profile (from homogeneous, $n = 0$, to mass point surrounded by a vanishing atmosphere, $n = 5$) and rotation (from spherical shape to fissional or equatorial breakup), but also in connection with mechanics (classical or relativistic) and the nature of the fluid (collisional or collisionless). To this last respect, it has been shown that any collisional polytrope has an exact collisionless counterpart within the range, $1/2 \leq n \leq 5$, (Vandervoort 1980; Vandervoort and Welty 1981); which implies a description of stellar systems and cluster of galaxies as well, with the extension to anisotropic stress tensors (Binney and Tremaine 1987, Chap. 4, §2). For further details, exhaustive presentation and complete references, an interested reader is addressed to specific textbooks (e.g., Horedt 2004).

In this view, the dependence of physical parameters on the polytropic index could be useful for a number of applications even if $n \geq 1/2$ for collisionless systems. For instance, liquid cores within planets or more exotic objects, such as neutron stars and quark stars, and deep oceans within satellites, could be described as polytropes with low n . Quasi static contraction via energy dissipation where total mass and angular momentum are left unchanged, while the polytropic index is increasing, could be described provided the dependence of selected physical parameters on n is known.

The isopycnic (i.e. constant density) surfaces can be approximated as similar and similarly placed ellipsoids (exact for homogeneous configurations) for several investigations, such as the description of gravitational radiation from collapsing and rotating massive star cores, (Saens and Shapiro 1978, 1981), rigidly rotating and binary polytropes, (Lai et al. 1993, 1994a,b), gravitational collapse of nonbaryonic dark matter and related pancake formation (Bisnovatyi-Kögan 2004, 2005), kinetic energy of ellipsoidal matter distributions (Rodrigues 2014). In short, inhomogeneous configurations can be described, to an acceptable extent, in terms of properties related to homogeneous configurations.

A description of tenuous gas-dust atmospheres of some stars and tenuous haloes surrounding compact elliptical galaxies, in terms of extended Roche configurations, is mentioned in a recent investigation (Kondratyev and Trubitsina 2013).

On the other hand, for reasons outlined above, the homogeneous ($n = 0$) and extended Roche ($n = 5$) limit for polytropes have never been attained (to the knowledge of the author) using numerical simulations where, at most, $0.1 \leq n \leq 4.9$. To this respect, a first step must necessarily be performed analytically.

The current attempt is restricted to the investigation of two specific

points, namely (i) the extent to which, for different density profiles and rotation rates, the C33 approximation (both in its original and extended form) is self-consistent in the sense that Eq. (3) is satisfied for an assumed tolerance equal to 10%, and (ii) the dependence on the polytropic index, shown by five physical parameters, which are selected in order to avoid divergence at the limiting configurations, $n = 0$ (homogeneous) and $n = 5$ (extended Roche system). More specifically, one among the above mentioned parameters is related to the nonrotating configuration, three to the rotating configuration, one to the onset of equatorial breakup.

The paper is organized as follows. The general theory of rigidly rotating polytropes is briefly outlined in Section 2. The dependence of the distortion index, $|\Delta\theta/\theta_w|$, on the polytropic index, n , $0 \leq n \leq 5$, the dimensionless radial coordinate, ξ , $0 \leq \xi \leq \Xi_E$, and the rotation parameter, v , $0 \leq v \leq v_R$, is determined in Section 3. Five selected physical parameters are plotted as a function of the polytropic index, n , in Section 4, where simple fitting functions are determined and relative errors are shown. The discussion is performed in Section 5. The conclusion is drawn in Section 6. Further analysis on slowly rotating isopycnic surfaces and detailed exposition of the fitting procedure are left to the Appendix.

2 General theory

The theory of rigidly rotating polytropes has been exhaustively developed in earlier attempts (e.g., Jeans 1929, Chap. IX; C33; C80; C83; Horedt 2004, Chap. 3); and shall not be repeated here, leaving aside extensions and improvements. An interested reader is addressed to the above quoted parent papers. Only what is relevant for the current investigation shall be reviewed in the following.

2.1 EC and EC associated equations

In dimensionless coordinates, the EC equation reads:

$$\frac{1}{\xi^2} \frac{\partial}{\partial \xi} \left(\xi^2 \frac{\partial \theta}{\partial \xi} \right) + \frac{1}{\xi^2} \frac{\partial}{\partial \mu} \left[(1 - \mu^2) \frac{\partial \theta}{\partial \mu} \right] - v = -\theta^n; \quad (4a)$$

$$\theta(0, \mu) = 1 \quad ; \quad \left(\frac{\partial \theta}{\partial \xi} \right)_{0, \mu} = 0 \quad ; \quad \left(\frac{\partial \theta}{\partial \mu} \right)_{0, \mu} = 0 \quad ; \quad (4b)$$

$$\lim_{v \rightarrow 0} \theta(\xi, \mu) = \theta_E(\xi_E) \quad ; \quad (4c)$$

where ξ is a dimensionless radial distance, $\delta = \arccos \mu$ the angle with respect to the rotation axis (polar angle), n the polytropic index ($0 \leq n \leq 5$), θ^n a

dimensionless density, v a dimensionless rotation parameter, and the index, E, denotes nonrotating configurations ($v = 0$).

The usual physical quantities relate to their dimensionless counterparts as:

$$r = \alpha\xi \quad ; \quad \alpha = \left[\frac{(n+1)p_c}{4\pi G\lambda^2} \right]^{1/2} = \left[\frac{(n+1)K\lambda^{1/n}}{4\pi G\lambda} \right]^{1/2} \quad ; \quad (5)$$

$$p = K\rho^{1+1/n} \quad ; \quad \rho = \lambda\theta^n \quad ; \quad (6)$$

$$v = \frac{\Omega^2}{2\pi G\lambda} \quad ; \quad (7)$$

where r is the radial distance, α a scaling radius, p the pressure, p_c the central pressure, ρ the density, λ the central density, K related to the central temperature, G the gravitation constant and Ω the angular velocity. For further details, an interested reader is addressed to earlier attempts (e.g., C33; C80).

The general solution to the EC equation, Eq. (4a), hereafter quoted as EC function, can be expanded in series of Legendre polynomials as:

$$\theta(\xi, \mu) = \sum_{\ell=0}^{+\infty} A_{2\ell} \theta_{2\ell}(\xi) P_{2\ell}(\mu) \quad ; \quad (8)$$

where odd terms are ruled out by symmetry with respect to the equatorial plane and $A_{2\ell}$ are coefficients which, for $2\ell > 0$, depend on the rotation parameter.

The boundary conditions related to the EC associated functions, $\theta_{2\ell}$, can be inferred from Eq. (4b) via (6) and (8). The result is:

$$\theta_{2\ell}(0) = \delta_{0,2\ell}; \quad \theta'_{2\ell}(0) = 0; \quad \lim_{v \rightarrow 0} \theta_0(\xi) = \theta_E(\xi_E); \quad (9)$$

$$A_0 = 1 \quad ; \quad \lim_{v \rightarrow 0} A_{2\ell}(v) = 0 \quad ; \quad 2\ell > 0 \quad ; \quad (10)$$

where δ_{ij} is the Kronecker symbol, not to be confused with the polar angle, $\delta = \arccos \mu$.

The Legendre polynomials, $P_\ell(\mu)$, can be expressed as:

$$P_\ell(\mu) = \frac{1}{2^\ell} \frac{1}{\ell!} \frac{d^\ell}{d\mu^\ell} [(\mu^2 - 1)^\ell] \quad ; \quad |P_\ell(\mu)| \leq 1 \quad ; \quad \ell = 0, 1, 2, \dots \quad ; \quad (11)$$

which satisfy the Legendre equations:

$$\frac{d}{d\mu} \left[(1 - \mu^2) \frac{dP_\ell}{d\mu} \right] = -\ell(\ell + 1) P_\ell(\mu) \quad ; \quad (12)$$

for non negative integer ℓ . For further details, an interested reader is addressed to classical textbooks on the theory of the potential (e.g., MacMillan 1930, Chap. VII, §§185-192).

If the distortion due to rigid rotation may be considered as a small perturbation with respect to the spherical shape, then the first term of the series expansion on the right-hand side of Eq. (8) is dominant and the power on the right-hand side of the EC equation, Eq. (4a), can safely be approximated as:

$$[\theta(\xi, \mu)]^n = [\theta_0(\xi)]^n + n[\theta_0(\xi)]^{n-1} \sum_{\ell=1}^{+\infty} A_{2\ell} \theta_{2\ell}(\xi) P_{2\ell}(\mu) ; \quad (13)$$

$$|\theta_0(\xi)| > \epsilon_0^* ; \quad (14)$$

which is a series expansion in Legendre polynomials, provided a fixed threshold, ϵ_0^* , is not exceeded.

The substitution of Eqs. (8) and (13) into the EC equation, Eq. (4a), taking separately the terms of same degree in Legendre polynomials, yields:

$$\frac{1}{\xi^2} \frac{d}{d\xi} \left(\xi^2 \frac{d\theta_{2\ell}}{d\xi} \right) - \frac{2\ell(2\ell+1)}{\xi^2} \theta_{2\ell} = \frac{\delta_{0,2\ell}}{A_{2\ell}} (-\theta_0^n + \nu) - (1 - \delta_{0,2\ell}) n \theta_0^{n-1} \theta_{2\ell}; \quad (15)$$

that is the EC associated equations of degree, 2ℓ . If $\theta_0 < 0$, the real part of the principal value of the complex power, $(\theta_0)^x$, has to be considered. For further details and exhaustive presentation, an interested reader is addressed to earlier attempts (Linnel 1981; C83; Geroyannis 1988; Geroyannis and Karageorgopoulos 2014).

2.2 Isopycnic surfaces

When a spherical polytrope attains rigid rotation, mass elements outside the rotation axis are displaced further away, yielding an oblate configuration where the polar axis coincides with the rotation axis. More specifically, oblateness weakens the gravitational force along the polar axis and strengthens the gravitational force along the equatorial plane, but the gravitational + centrifugal force is also weakened, which implies loss of spherical shape.

Let $\theta_E(\xi_E) = \kappa$ and $\theta(\xi, \mu) = \kappa$ be a generic isopycnic surface related to the nonrotating and rigidly rotating configuration, respectively. In terms of the dimensionless radial coordinate, ξ , the isopycnic surface can be expressed as $\xi = \xi_E$ and $\xi = \xi(\mu)$, respectively. Let the polar and the equatorial coordinate be denoted as $\xi_p = \xi(1)$ and $\xi_e = \xi(0)$, respectively, where oblateness implies $\xi_p \leq \xi_E \leq \xi_e$.

The generic oblate isopycnic surface, via Eqs. (8), (9), (10), reads:

$$\theta(\xi, \mu) = \theta_0(\xi) + R_1(\xi, \mu) = \kappa \ ; \quad (16)$$

$$R_1(\xi, \mu) = \sum_{\ell=1}^{+\infty} A_{2\ell} \theta_{2\ell}(\xi) P_{2\ell}(\mu) \ ; \quad (17)$$

where $\xi_p \leq \xi \leq \xi_e$ owing to oblateness. In addition, the following inequality:

$$|R_1(\xi, \mu)| \ll \epsilon_0^* < |\theta_0(\xi)| \ ; \quad (18)$$

implies the validity of Eq. (13). The middle side of Eq. (16) describes an expansion of the nonrotating polytrope as a whole, via θ_0 , and superimposed on this an oblateness, via R_1 . More specifically, θ_0 relates to an expanded sphere, where the radial contribution of rigid rotation adds to the undistorted configuration, and R_1 quantifies the meridional distortion.

Let ξ_0 define the (fictitious) isopycnic surface of the expanded sphere, as:

$$\theta_0(\xi_0) = \theta_E(\xi_E) = \kappa \ ; \quad (19)$$

where radial expansion implies $\xi_E \leq \xi_0$. The substitution of Eq. (19) into (16) yields:

$$R_1(\xi_0, \mp \mu_0) = 0 \ ; \quad (20)$$

and the locus, $(\xi_0, \mp \mu_0)$, defines the intersection between the oblate isopycnic surface, $\theta(\xi, \mu) = \kappa$, and the (fictitious) isopycnic surface, $\theta_0(\xi_0) = \kappa$, as depicted in Fig. 1. In the nonrotating limit, $v \rightarrow 0$, $\xi_0 \rightarrow \xi_E$, and the term containing $P_2(\mu)$ is expected to be dominant with respect to the others in Eq. (17). Accordingly, μ_0 relates to $P_2(\mu) = 0$, hence $\mu_0 \rightarrow 1/\sqrt{3}$. For further details, an interested reader is addressed to Appendix A.

2.3 Gravitational potential

The gravitational potential within EC polytropes reads (e.g., C80):

$$\mathcal{V}_G(\xi, \mu) = 4\pi G \lambda \alpha^2 \left\{ \theta(\xi, \mu) - \frac{1}{6} v \xi^2 [1 - P_2(\mu)] \right\} + \mathcal{V}_p \ ; \quad (21)$$

where \mathcal{V}_p is an additive constant which, at the moment, remains undetermined.

The substitution of Eq. (8) into (21) yields:

$$\mathcal{V}_G(\xi, \mu) = 4\pi G \lambda \alpha^2 \sum_{\ell=0}^{+\infty} \left[A_{2\ell} \theta_{2\ell}(\xi) - \frac{\delta_{2\ell,0} - \delta_{2\ell,2}}{6} v \xi^2 \right] P_{2\ell}(\mu) + \mathcal{V}_p \ ; \quad (22)$$

where $A_0 = 1$ according to Eq. (10).

The gravitational potential of a body of revolution, at sufficiently large distance outside the boundary, can be expressed as (e.g., MacMillan 1930, Chap. VII, §193):

$$\mathcal{V}_G(\xi, \mu) = 4\pi G\lambda\alpha^2 \sum_{\ell=0}^{+\infty} \frac{c_{2\ell}}{\xi^{2\ell+1}} P_{2\ell}(\mu) \quad ; \quad \xi \gg \Xi \quad ; \quad (23)$$

where $c_{2\ell}$ are dimensionless coefficients and the odd terms are ruled out by symmetry with respect to the equatorial plane.

For points near the boundary, Eq. (23) is exact only for spherical-symmetric matter distributions and Roche systems, but remains acceptable provided oblateness maintains sufficiently small or concentration maintains sufficiently high. The worst case relates to homogeneous configurations ($n = 0$) where, on the other hand, the gravitational potential may be expressed analytically (e.g., MacMillan 1930, Chap. II, §39). The best case relates to extended Roche systems ($n = 5$), where either the boundary is infinitely distant from the centre of mass or the whole mass is concentrated at a single point surrounded by a massless atmosphere filling a finite volume, both implying an exact formulation.

The continuity of the gravitational potential and the gravitational force on a selected point of the boundary, $\Xi = \Xi(\mu)$, implies Eqs. (22), (23), and related first derivatives, match at (Ξ, μ) for the terms of the same degree in Legendre polynomials. The result is:

$$A_{2\ell}\theta_{2\ell}(\Xi) - \frac{\delta_{2\ell,0} - \delta_{2\ell,2}}{6} v\Xi^2 + \delta_{2\ell,0}c_p = \frac{c_{2\ell}}{\Xi^{2\ell+1}} \quad ; \quad (24)$$

$$A_{2\ell}\theta'_{2\ell}(\Xi) - \frac{\delta_{2\ell,0} - \delta_{2\ell,2}}{3} v\Xi = -\frac{(2\ell+1)c_{2\ell}}{\Xi^{2\ell+2}} \quad ; \quad (25)$$

$$c_p = \frac{\mathcal{V}_p}{4\pi G\lambda\alpha^2} \quad ; \quad (26)$$

where $A_0 = 1$, Eq. (10), and the constants, $A_{2\ell}$, $c_{2\ell}$, c_p , are the solutions of the system, Eqs. (24) and (25), for $2\ell = 0, 2, 4, \dots$

After performing a lot of algebra, related explicit expressions read:

$$c_p = -\theta_0(\Xi) - \Xi\theta'_0(\Xi) + \frac{1}{2}v\Xi^2 \quad ; \quad (27)$$

$$c_0 = -\Xi^2\theta'_0(\Xi) + \frac{1}{3}v\Xi^3 \quad ; \quad (28)$$

for $2\ell = 0$ where, in general, $\theta_0(\Xi) = \kappa_b$, and:

$$A_2 = -\frac{5}{6} \frac{v\Xi^2}{3\theta_2(\Xi) + \Xi\theta'_2(\Xi)} \quad ; \quad (29)$$

$$c_2 = -\frac{\nu}{6} \frac{\Xi^5 [2\theta_2(\Xi) - \Xi\theta_2'(\Xi)]}{3\theta_2(\Xi) + \Xi\theta_2'(\Xi)} = \frac{1}{5} A_2 \Xi^3 [2\theta_2(\Xi) - \Xi\theta_2'(\Xi)] ; \quad (30)$$

for $2\ell = 2$, and:

$$A_{2\ell} [(2\ell + 1)\theta_{2\ell}(\Xi) + \Xi\theta_{2\ell}'(\Xi)] = 0 ; \quad (31)$$

which implies the following:

$$A_{2\ell} = 0 ; \quad c_{2\ell} = 0 ; \quad (32)$$

for $2\ell > 2$. More specifically, a null value of the sum within square brackets in Eq. (31) would be in contradiction with the EC associated equation, Eq. (15).

Accordingly, Eqs. (16), (17), (18), reduce to:

$$\theta(\xi, \mu) = \theta_0(\xi) + A_2 \theta_2(\xi) P_2(\mu) = \kappa ; \quad (33)$$

$$R_1(\xi, \mu) = A_2 \theta_2(\xi) P_2(\mu) ; \quad (34)$$

$$|A_2 \theta_2(\xi) P_2(\mu)| \ll \epsilon_0^* < |\theta_0(\xi)| ; \quad (35)$$

where, in particular, $\kappa = \kappa_b$ on the boundary. In addition, Eq. (20) reduces to:

$$A_2 \theta_2(\xi_0) P_2(\mp \mu_0) = 0 ; \quad (36)$$

which implies $\mu_0 = 1/\sqrt{3}$, $\delta_0 = \arctan \sqrt{2}$, and the locus of intersections between isopycnic surfaces, $\theta(\xi, \mu) = \kappa$ and $\theta_0(\xi_0) = \kappa$, is the surface of a cone with axis coinciding with the polar axis, vertex coinciding with the centre of mass and generatrixes, $\delta_0 = \arctan \sqrt{2}$.

If, in particular, $\Xi = \Xi_p$ in Eqs. (27)-(31), the equation of the boundary via Eq. (33) specifies to:

$$\theta(\Xi_p, 1) = \theta_0(\Xi_p) + A_2 \theta_2(\Xi_p) P_2(1) = \kappa_b ; \quad (37)$$

where $P_2(1) = 1$. Then the combination of Eqs. (29) and (37) yields:

$$\frac{5}{6} \frac{\nu \Xi_p^2}{3\theta_2(\Xi_p) + \Xi_p \theta_2'(\Xi_p)} = \frac{\theta_0(\Xi_p) - \kappa_b}{\theta_2(\Xi_p)} ; \quad (38)$$

which is a transcendental equation in Ξ_p . Keeping in mind $\theta_2(\xi) \sim \xi^2$ as $\xi \rightarrow 0$ (C33; C83) and $\theta_0(\Xi_0) = \kappa_b$, $\Xi_0 \geq \Xi_p$, the left-hand side of Eq. (38) maintains both finite and positive, while the right-hand side is monotonically decreasing from positive infinite to zero via Eqs. (9) and (19), within the range, $0 \leq \Xi_p \leq \Xi_0$. Accordingly, Eq. (37) admits a unique solution within the above mentioned range.

The dimensionless equatorial semiaxis, Ξ_e , can be determined using the equation of the boundary via Eq. (33), which translates into:

$$\theta(\Xi_e, 0) = \theta_0(\Xi_e) + A_2\theta_2(\Xi_e)P_2(0) = \kappa_b \quad ; \quad (39)$$

where $P_2(0) = -1/2$, which is a transcendental equation in Ξ_e . The knowledge of the dimensionless semiaxes, Ξ_p, Ξ_e , implies the knowledge of the axis ratio, as:

$$\epsilon = \frac{\alpha\Xi_p}{\alpha\Xi_e} = \frac{\Xi_p}{\Xi_e} \quad ; \quad (40)$$

according to Eq. (5).

In the following, the whole procedure for determining A_2 and related quantities via Eq. (29), particularized to $\Xi = \Xi_p$, shall be quoted as the Chandrasekhar procedure (C33) extended to the pole of the system or, in short, the extended C33 procedure.

If the isopycnic surfaces are expressed by Eq. (33), a better method for determining the constants, c_p and A_2 , acts as follows: (1) calculate the gravitational potential at the centre of mass using the equilibrium equation via Eq. (21) and the mass distribution via Eq. (6), and express c_p by comparison of related results; (2) calculate the gravitational force at the pole using the equilibrium equation via Eq. (21) and the mass distribution via Eq. (6), and express A_2 by comparison of related results. For further details, an interested reader is addressed to the parent papers (C80; C83).

In the following, the whole procedure for determining A_2 and related quantities, as outlined above, shall be quoted as the C80 procedure.

2.4 C33 approximation

A simpler approximation was used in the original parent paper (C33). More specifically, Eq. (8) is expressed therein as:

$$\theta(\xi, \mu) = \theta_E(\xi) + vR_0(\xi, \mu) \quad ; \quad (41)$$

$$R_0(\xi, \mu) = \sum_{\ell=0}^{+\infty} C_{2\ell}\psi_{2\ell}(\xi)P_{2\ell}(\mu) \quad ; \quad (42)$$

$$C_0 = 1 \quad ; \quad \psi_{2\ell}(0) = 0 \quad ; \quad \psi'_{2\ell}(0) = 0 \quad ; \quad (43)$$

where $C_{2\ell}$ are constants and $\xi_p \leq \xi \leq \xi_e$ on a selected isopycnic surface.

If the distortion due to rigid rotation may be considered as a small perturbation with respect to the spherical shape, then the first term of the series expansion on the right-hand side of Eq. (41) is dominant and the power on

the right-hand side of the EC equation, Eq. (4a), can safely be approximated as:

$$[\theta(\xi, \mu)]^n = [\theta_E(\xi)]^n + n[\theta_E(\xi)]^{n-1} \nu \sum_{\ell=0}^{+\infty} C_{2\ell} \psi_{2\ell}(\xi) P_{2\ell}(\mu) ; \quad (44)$$

$$|\theta_E(\xi)| > \epsilon_E^* ; \quad (45)$$

which is a series expansion in Legendre polynomials, provided a fixed threshold, ϵ_E^* , is not exceeded.

The substitution of Eqs. (41) and (44) into the EC equation, Eq. (4a), taking separately the terms of same degree in Legendre polynomials, yields:

$$\frac{1}{\xi^2} \frac{d}{d\xi} \left(\xi^2 \frac{d\psi_{2\ell}}{d\xi} \right) - \frac{2\ell(2\ell+1)}{\xi^2} \psi_{2\ell} = \delta_{2\ell,0} - n\theta_E^{n-1} \psi_{2\ell} ; \quad (46)$$

where ψ_0 and $\psi_{2\ell}$, $2\ell > 0$, relate to the radial expansion and the meridional distortion, respectively, due to rigid rotation. The comparison between Eqs. (15) and (46) discloses that:

$$\psi_0(\xi) = \lim_{\nu \rightarrow 0} \frac{\theta_0(\xi, \nu) - \theta_E(\xi)}{\nu} ; \quad (47)$$

$$\begin{aligned} \lim_{\nu \rightarrow 0} [\theta_0(\xi, \nu)]^n &= \lim_{\nu \rightarrow 0} [\theta_E(\xi) + \nu\psi_0(\xi)]^n \\ &= \lim_{\nu \rightarrow 0} \{ [\theta_E(\xi)]^n + n[\theta_E(\xi)]^{n-1} \nu\psi_0(\xi) \} ; \end{aligned} \quad (48)$$

$$C_{2\ell} \psi_{2\ell}(\xi) = \lim_{\nu \rightarrow 0} \frac{A_{2\ell}(\nu) \theta_{2\ell}(\xi, \nu)}{\nu} ; \quad 2\ell > 0 ; \quad (49)$$

which enlightens the difference between C33 and extended C33 approximation.

Keeping in mind the solutions of EC associated equations, Eqs. (15) and (46), remain undetermined by a multiplicative constant for $2\ell > 0$, Eq. (49) may be splitted as:

$$C_{2\ell} = \lim_{\nu \rightarrow 0} \frac{A_{2\ell}(\nu)}{\nu} ; \quad \psi_{2\ell}(\xi) = \lim_{\nu \rightarrow 0} \theta_{2\ell}(\xi, \nu) ; \quad 2\ell > 0 ; \quad (50)$$

with no loss of generality.

The gravitational potential and the gravitational force inside and outside the system can be matched on the boundary of the nonrotating sphere, $\Xi = \Xi_E$, and Eqs. (27)-(32) still hold provided Ξ_p , θ_0 , $A_{2\ell}\theta_{2\ell}$, are replaced by Ξ_E , $\theta_E + \nu\psi_0$, $\nu C_{2\ell}\psi_{2\ell}$, respectively. The result is:

$$c_p = c_{pE} + \nu d_p ; \quad c_{pE} = -\theta_E(\Xi_E) - \Xi_E \theta'_E(\Xi_E) ;$$

$$d_p = -\psi_0(\Xi_E) - \Xi_E \psi'_0(\Xi_E) + \frac{1}{2} \Xi_E^2 ; \quad (51)$$

$$c_0 = c_E + v d_0 ; \quad c_E = -\Xi_E^2 \theta'_E(\Xi_E) ;$$

$$d_0 = -\Xi_E^2 \psi'_0(\Xi_E) + \frac{1}{3} \Xi_E^3 ; \quad (52)$$

$$A_2 = v C_2 ; \quad C_2 = -\frac{5}{6} \frac{\Xi_E^2}{3\psi_2(\Xi_E) + \Xi_E \psi'_2(\Xi_E)} ; \quad (53)$$

$$c_2 = v d_2 ; \quad d_2 = \frac{1}{5} C_2 \Xi_E^3 [2\psi_2(\Xi_E) - \Xi_E \psi'_2(\Xi_E)] ; \quad (54)$$

$$C_{2\ell} = 0 ; \quad d_{2\ell} = 0 ; \quad 2\ell > 2 ; \quad (55)$$

for further details, an interested reader is addressed to the parent paper (C33).

In the following, the whole procedure for determining $A_2 = v C_2$ and related quantities by use of the Chandrasekhar approximation (C33) shall be quoted as the C33 procedure.

3 A self-consistent method

The validity of the EC associated equations, Eq. (15), via Eq. (13), is implied by the inequality, expressed by Eq. (35). For a generic isopycnic surface, defined by Eq. (33), the above mentioned inequality can be formulated as:

$$\zeta(\xi, \mu) \ll 1 ; \quad (56)$$

$$\zeta(\xi, \mu) = \left| \frac{A_2 \theta_2(\xi) P_2(\mu)}{\theta_0(\xi)} \right| = \left| \frac{\theta_0(\xi_0)}{\theta_0(\xi)} - 1 \right| ; \quad (57)$$

where $\theta_0(\xi_0) = \kappa$ and $\xi_0 = \xi(\mp 1/\sqrt{3})$ is the intersection between a selected oblate isopycnic surface and its (fictitious) counterpart related to the expanded sphere. The function, $\zeta(\xi, \mu)$, may be conceived as a distortion indicator. In particular, $\zeta(\xi_0, \mu_0) = 0$ and $\zeta(\Xi, \mu) = 1$ provided $\Xi \neq \Xi_0$ and $\kappa_b = 0$. For fixed ξ , the distortion indicator has a maximum on the polar axis, $\zeta(\xi, \mu) \leq \zeta(\xi_p, 1) = \zeta_p(\xi_p)$, due to $P_2(\mu) \leq 1$. According to Eq. (57), the distortion indicator, ζ_p , is maximized as $\kappa_b = \theta_0(\Xi_0) \rightarrow 0$ or $\theta(\Xi, \mu) \rightarrow 0$ which, on the other hand, is mostly considered in literature (e.g., Horedt 2004, Chap. 2, §2.2). For this reason, $\kappa_b = 0$ shall be assumed in the following. To get deeper insight, special cases for which analytical solutions exist shall first be considered.

3.1 The special case $n = 0$

The solutions of the EC associated equations, Eqs. (15), (46), for $n = 0$, keeping in mind Eqs. (47), (50), read:

$$\theta_0(\xi) = 1 - \frac{1-v}{6}\xi^2 ; \quad (58)$$

$$\Xi_0 = \frac{\Xi_E}{(1-v)^{1/2}} = \left(\frac{6}{1-v}\right)^{1/2} ; \quad (59)$$

$$\psi_0(\xi) = \lim_{v \rightarrow 0} \frac{\theta_0(\xi) - \theta_E(\xi)}{v} = \frac{1}{6}\xi^2 ; \quad (60)$$

$$\theta_2(\xi) = \psi_2(\xi) = \xi^2 ; \quad (61)$$

where the boundary conditions are expressed by Eq. (9).

According to the extended C33 procedure, Eq. (29) reduces to:

$$A_2 = -\frac{1}{6}v ; \quad (62)$$

and the substitution of Eqs. (58)-(62) into (37)-(40) yields after some algebra:

$$\begin{aligned} \Xi_p &= \Xi_E ; \quad \Xi_e = \Xi_E \left(1 - \frac{3}{2}v\right)^{-1/2} ; \quad \Xi_E = \sqrt{6} ; \\ \epsilon &= \left(1 - \frac{3}{2}v\right)^{1/2} ; \end{aligned} \quad (63)$$

accordingly, the rotation parameter, v , the dimensionless radius of the expanded sphere, Ξ_0 , and the coefficient, A_2 , may be expressed in terms of the axis ratio, ϵ , as:

$$v = (1 - \epsilon^2)\gamma(1) ; \quad (64)$$

$$\Xi_0 = \Xi_E \left(\frac{3}{1 + 2\epsilon^2}\right)^{1/2} ; \quad (65)$$

$$A_2 = -\frac{1 - \epsilon^2}{6}\gamma(1) ; \quad (66)$$

where $\gamma(1) = 2/3$, according to the next Eq. (68). The above results cannot be considered as acceptable approximations, leaving aside the dependence of A_2 on ϵ , Eq. (66), which shows an increasing discrepancy for decreasing ϵ up to 30% for $\epsilon = 0$ (C80).

An exact formulation can be derived following the C80 procedure. The result is:

$$A_2 = -\frac{1 - \epsilon^2}{6}\gamma(\epsilon) ; \quad \epsilon = \frac{\Xi_p}{\Xi_e} ; \quad (67)$$

$$\gamma(\epsilon) = \frac{2}{1 - \epsilon^2} \left[1 - \epsilon \frac{\arcsin \sqrt{1 - \epsilon^2}}{\sqrt{1 - \epsilon^2}} \right] ;$$

$$\gamma(1) = \frac{2}{3} ; \quad \gamma(0) = 2 ; \quad (68)$$

$$\frac{d\gamma}{d\epsilon} = \frac{1}{1 - \epsilon^2} \left[(1 + 2\epsilon^2) \frac{\gamma}{\epsilon} - \frac{2}{\epsilon} \right] ; \quad (69)$$

$$v(\epsilon) = 1 - \frac{1 + 2\epsilon^2}{2} \gamma(\epsilon) ; \quad v(1) = v(0) = 0 ; \quad (70)$$

accordingly, $v(\epsilon)$ is nonmonotonic and $A_2(1) = 0$, $A_2(0) = -1/3$.

The coordinates of the extremum point, which must necessarily be positive, satisfy the transcendental equation, $dv/d\epsilon = 0$, or (e.g., Caimmi 2006):

$$\gamma(\epsilon) = 2 \frac{1 + 2\epsilon^2}{1 + 8\epsilon^2} ; \quad (71)$$

which has two solutions on the boundary of the domain, according to Eq. (68), and a third solution inside the domain, related to the extremum point (e.g., Chandrasekhar 1969, Chap. 5, §32). The flat configuration, $\epsilon = 0$, $v = 0$, is also centrifugally supported, $v_R = 0$, but the system is unstable towards bar modes for $\epsilon < 0.58272$. For further details and additional references, an interested reader is addressed to the parent paper (C80).

The substitution of Eqs. (58)-(61) and (66) into (57) yields after some algebra:

$$\zeta(\xi, \mu) = \left| \frac{\xi^2 - \xi_0^2}{\Xi_0^2 - \xi^2} \right| ; \quad (72)$$

where it can be seen $\zeta(\xi, \mu) \ll 1$ implies $\xi_0 \ll \Xi_0$ inside the related isopycnic surface of the expanded sphere, $\xi < \xi_0$, and $\xi \ll [(\Xi_0^2 + \xi_0^2)/2]^{1/2}$ outside the related isopycnic surface of the expanded sphere but inside the expanded sphere, $\xi_0 < \xi < \Xi_0$, while no acceptable solution to the above mentioned inequality exists outside the expanded sphere, $\xi > \Xi_0$.

For practical purposes, it is better dealing with the upper limit, $\zeta_p(\xi_p) = \zeta(\xi_p, 1) \geq \zeta(\xi, \mu)$. To this respect, the substitution of Eqs. (58), (61) and (62) or (67) into (57) yields, after some algebra, an explicit expression of the distortion indicator, ζ_p , for the extended C33 or the C80 procedure, respectively.

3.2 The special case $n = 1$

The solutions of the EC associated equations, Eqs. (15), (46), for $n = 1$, keeping in mind Eqs. (47), (50), read²:

$$\theta_0(\xi) = (1 - v) \frac{\sin \xi}{\xi} + v ; \quad (73)$$

$$\psi_0(\xi) = \lim_{v \rightarrow 0} \frac{\theta_0(\xi) - \theta_E(\xi)}{v} = 1 - \frac{\sin \xi}{\xi} ; \quad (74)$$

$$\theta_2(\xi) = \psi_2(\xi) = 15 \left[\left(\frac{3}{\xi^2} - 1 \right) \frac{\sin \xi}{\xi} - \frac{3 \cos \xi}{\xi} \right] ; \quad (75)$$

where the boundary conditions are expressed by Eq. (9). The first derivative of the last function, after some algebra, reads:

$$\begin{aligned} \theta_2'(\xi) &= \psi_2'(\xi) \\ &= 15 \left[\left(\frac{9}{\xi^3} + \frac{4}{\xi} \right) \frac{\sin \xi}{\xi} + \left(\frac{9}{\xi^2} - 1 \right) \frac{\cos \xi}{\xi} \right] ; \end{aligned} \quad (76)$$

and the substitution of Eqs. (75), (76), into (29), according to the extended C33 procedure, after some algebra yields:

$$A_2 = -\frac{v \Xi^2}{18} \left[\left(\frac{18}{\Xi^2} + 1 \right) \frac{\sin \Xi}{\Xi} - \cos \Xi \right]^{-1} ; \quad (77)$$

and the dimensionless semiaxes, Ξ_p , Ξ_e , are the solution of the transcendental equations, Eqs. (38), (39), respectively, via (73), taking $\kappa_b = 0$.

Numerical computations must be performed following the C80 procedure, as the gravitational potential within the system cannot be expressed analytically. It can be seen the rotation parameter, v , and the coefficient, $-A_2$, monotonically increase up to about 0.107 and 0.962, respectively, as the axis ratio, ϵ , decreases up to about 0.531. Additional rotation would imply equatorial breakup. For further details, an interested reader is addressed to the parent paper (C80).

3.3 The special case $n = 5$

The solutions of the EC associated equations, Eqs. (15), (46), for $n = 5$, keeping in mind Eqs. (47), (50), read:

$$\theta_0(\xi) = \cos \nu + \frac{1}{2} v \tan^2 \nu ; \quad \nu = \arctan \frac{\xi}{\sqrt{3}} ; \quad (78)$$

² It is worth noticing the associated EC function, $\theta_2(\xi)$, is lacking of the factor, 15, in the parent paper (C80) which, on the other hand, is absorbed by the constant, A_2 (B_2 therein), leaving the results unchanged. Conversely, the factor, 15, appears in a subsequent attempt (C83).

$$\psi_0(\xi) = \lim_{\nu \rightarrow 0} \frac{\theta_0(\xi) - \theta_E(\xi)}{\nu} = \frac{1}{2} \tan^2 \nu \quad ; \quad (79)$$

$$\theta_2(\xi) = \psi_2(\xi) = \frac{15}{128} \left\{ \frac{3[\nu - \sin \nu \cos^3 \nu + \sin^3 \nu \cos \nu]}{\sin^3 \nu \cos^2 \nu} - \frac{8[\sin^3 \nu \cos^5 \nu - \sin^5 \nu \cos^3 \nu]}{\sin^3 \nu \cos^2 \nu} \right\} ; \quad (80)$$

where the boundary conditions are expressed by Eq. (9).

With regard to Eqs. (78)-(79), it can be seen $\theta_E(\xi) = \cos \nu$ fits to the correct nonrotating limit (e.g., C80) while $\psi_0(\xi) = (1/2) \tan^2 \nu$ is an approximate solution of Eq. (46) which attains the same asymptotic expression as the exact solution, $\psi_0(\xi) \rightarrow \xi^2/6$, for both $\xi \rightarrow 0$ and $\xi \rightarrow +\infty$ (H90). On the other hand, $\nu \rightarrow 0$ in the case under discussion and $\nu\psi_0(\xi)$ is infinitesimal while $\theta_E(\xi)$ maintains finite provided $\xi < +\infty$. Accordingly, Eq. (78) may be considered as infinitely close to the exact solution of the EC associated equation of degree, $2\ell = 0$, Eq. (15).

In the limit, $\xi \rightarrow +\infty$, the following relations hold:

$$\lim_{\xi \rightarrow +\infty} \left[\xi \theta_0(\xi) - \frac{1}{6} \nu \xi^3 \right] = \sqrt{3} \quad ; \quad (81)$$

$$\lim_{\xi \rightarrow +\infty} \left[\xi^2 \theta'_0(\xi) - \frac{1}{3} \nu \xi^3 \right] = -\sqrt{3} \quad ; \quad (82)$$

$$\lim_{\xi \rightarrow +\infty} \left[\xi^3 \theta''_0(\xi) - \frac{1}{3} \nu \xi^3 \right] = 2\sqrt{3} \quad ; \quad (83)$$

$$\lim_{\xi \rightarrow +\infty} \left[\xi^{-2} \theta_2(\xi) \right] = \frac{15\pi}{256} \quad ; \quad (84)$$

$$\lim_{\xi \rightarrow +\infty} \left[\xi^{-1} \theta'_2(\xi) \right] = \frac{15\pi}{128} \quad ; \quad (85)$$

$$\lim_{\xi \rightarrow +\infty} \theta''_2(\xi) = \frac{15\pi}{128} \quad ; \quad (86)$$

$$\lim_{\xi \rightarrow +\infty} [2\theta_2(\xi) - \xi \theta'_2(\xi)] = \frac{225\pi}{256} \quad ; \quad (87)$$

where the dimensionless boundary, $\Xi(\mu)$, extends to infinity and $\kappa_b = 0$.

In the nonrotating limit, $\nu \rightarrow 0$, $\theta_0(\xi) \rightarrow \theta_E(\xi)$, Eqs. (81)-(83) reduce to:

$$\lim_{\xi \rightarrow +\infty} [\xi \theta_E(\xi)] = \sqrt{3} \quad ; \quad (88)$$

$$\lim_{\xi \rightarrow +\infty} [\xi^2 \theta'_E(\xi)] = -\sqrt{3} \quad ; \quad (89)$$

$$\lim_{\xi \rightarrow +\infty} [\xi^3 \theta''_E(\xi)] = 2\sqrt{3} \quad ; \quad (90)$$

where the dimensionless boundary, $\Xi_E(\mu)$, attains infinity.

According to the extended C33 procedure, Eqs. (27)-(30) reduce to:

$$c_p = 0 \quad ; \quad c_0 = \sqrt{3} \quad ; \quad A_2 = -\frac{128}{45\pi}v \quad ; \quad c_2 = -\frac{1}{2}v\Xi^3 \quad ; \quad (91)$$

and the substitution of Eqs. (78)-(91) into (37)-(40) after some algebra yields:

$$\Xi_p = \Xi_E \quad ; \quad \Xi_e = \frac{\Xi_E}{\epsilon} \quad ; \quad (92)$$

$$v\Xi_E^3 = 4\sqrt{3}\epsilon^2(1 - \epsilon) \quad ; \quad (93)$$

$$v\Xi_e^3 = 4\sqrt{3}\frac{1 - \epsilon}{\epsilon} \quad ; \quad (94)$$

where, in particular, centrifugal equilibrium is attained at the equator for $v\Xi_e^3 = 2\sqrt{3}$, which implies $\epsilon = 2/3$, $v_R\Xi_E^3 = 16\sqrt{3}/27$. Additional rotation makes the onset of equatorial breakup. For further details, an interested reader is addressed to the parent paper (C87).

The substitution of Eqs. (78)-(80) and (91) into (57), keeping in mind $\epsilon \geq 2/3$, yields after some algebra:

$$\zeta(\xi, \mu) = \left| \frac{\sqrt{3}/\xi_0 + v\xi_0^2/6}{\sqrt{3}/\xi + v\xi^2/6} \right| \quad ; \quad (95)$$

for infinite dimensionless distances, $\xi \rightarrow +\infty$; if otherwise, $\zeta(\xi, \mu) \rightarrow 0$.

For practical purposes, it is better dealing with the upper limit, $\zeta_p(\xi_p) = \zeta(\xi_p, 1) \geq \zeta(\xi, \mu)$. To this respect, the substitution of Eqs. (81), (84), (91)-(94), into (57) yields after some algebra:

$$\zeta_p(\xi_p) = \zeta(\xi_p, 1) = \left\{ 1 + \left[\frac{2}{3}\epsilon^2(1 - \epsilon)\frac{\xi_p}{\Xi_E} \right]^{-1} \right\}^{-1} \quad ; \quad (96)$$

provided $\xi_p \rightarrow +\infty$. The special case of centrifugal equilibrium, $\epsilon = 2/3$, at the pole, $\xi_p = \Xi_p = \Xi_E$, reads $\zeta(\Xi_E, 1) = 8/89$.

The above results can be obtained following the C80 procedure which, in the case under discussion, is equivalent to the extended C33 procedure, in that both are exact. For further details, an interested reader is addressed to the parent paper (C87).

3.4 The general case

Equilibrium configurations related to both C33 and extended C33 procedure are increasingly near to their exact counterparts as the rotation parameter is

increasingly smaller, $v \rightarrow 0$. On the other hand, equilibrium configurations related to the C80 procedure are conceptually exact but suffer from approximations related to numerical integrations. In particular, v is infinitesimal for $n = 5$, where the isopycnic surfaces are distorted only at infinite dimensionless distances from the centre of mass, $\xi \rightarrow +\infty$, and the extended C33 procedure yields exact results.

Conversely, v rises up to a maximum and later decreases for $n = 0$, where the isopycnic surfaces (intended as coinciding with gravitational + centrifugal equipotential surfaces for homogeneous configurations) can be distorted, leaving aside instabilities, up to a flat disk, and the extended C33 procedure yields very rough results unless $v \rightarrow 0$, $\epsilon \rightarrow 1$.

The special case, $n = 1$, lies between the above mentioned extreme situations, $n = 5$ and $n = 0$. Accordingly, results from both the C33 and the extended C33 procedure are expected to provide a better description of equilibrium configurations for increasing polytropic index, n .

Aiming to a rapid insight to the dependence of the distortion indicator, ζ_p , on the polytropic index, n , and the rotation parameter, v , the EC associated functions, θ_0 , θ_2 , shall be expressed according to the extended C33 procedure, but approximated according to the C33 procedure. The result is:

$$\theta_0(\xi, v) = \theta_E(\xi) + v\psi_0(\xi) \quad ; \quad (97)$$

$$A_2\theta_2(\xi, v) = vC_2\psi_2(\xi) \quad ; \quad (98)$$

$$C_2 = \frac{A_2}{v} \quad ; \quad (99)$$

and the substitution of Eqs. (33), (97), (98), into (57) yields after some algebra:

$$\zeta(\xi, \mu) \leq \zeta(\xi_p, 1) = \zeta_p(\xi_p) = \left| \frac{vC_2\psi_2(\xi)}{\theta_E(\xi) + v\psi_0(\xi)} \right| \ll 1 \quad ; \quad (100)$$

which may readily be calculated in that the functions, θ_E , ψ_0 , ψ_2 , are tabulated.

On the boundary of the nonrotating sphere, $\xi = \Xi_E$, $\theta_E(\Xi_E) = 0$, high-precision values of Ξ_E , $\theta'_E(\Xi_E)$, $\psi_0(\Xi_E)$, $\psi'_0(\Xi_E)$, $\psi_2(\Xi_E)$, $\psi'_2(\Xi_E)$, are available (e.g., C85; H90). In addition, $\zeta_p(\Xi_E) = -C_2\psi_2(\Xi_E)/\psi_0(\Xi_E)$, regardless of the rotation parameter, v , with the exception of the special case, $n = 5$, where $\theta_E(\xi)$, $v\psi_0(\xi)$, $v\psi_2(\xi)$, are infinitesimal of the same order for $\xi \rightarrow \Xi_E$, as can be inferred from Eqs. (81)-(86). High-precision values of $\theta_E(\xi)$, $0 \leq \xi \leq \Xi_E$, are also available (e.g., Horedt 1986). On the other hand, to the knowledge of the author, values of $\psi_0(\xi)$, $\psi'_0(\xi)$, $\psi_2(\xi)$, $\psi'_2(\xi)$, $0 < \xi < \Xi_E$, can be found only in the parent paper (C33). The above mentioned references make

the source of the data used for analysing the dependence of the distortion indicator, $\zeta_p(\xi_p)$, on the polytropic index, n , the rotation parameter, v , and the fractional dimensionless radial coordinate, ξ/Ξ_E .

The results are shown in Figs. 2 and 3, where different curves (from bottom to top) relate to rotation parameter values, $v/v_c = 0.1, 0.2, \dots, 1.0$, and v_c is a threshold which denotes the onset of instability against bar modes ($n \lesssim 0.808$) or equatorial breakup ($n \gtrsim 0.808$). To gain insight, cases $n = 1, 5$, are repeated and the special value, $\zeta_p = 0.1$, is marked by a dashed horizontal straight line. More specifically, left and right panels of Fig. 2 correspond to the C80 and C33 procedure, respectively, while only the latter is considered in Fig. 3. All curves diverge at $\xi = \Xi_0$, $\theta_0(\Xi_0) = 0$, according to Eq. (57), provided $\mu \neq \mu_0$ and $n < 5$. The parameter, $C_2 = A_2/v$, is independent of the rotation parameter, v , according to Eq. (53), in the C33 procedure, while the contrary holds, according to Eqs. (67), (70), for $n = 0$, and to numerical results for $0 < n < 5$, in the C80 procedure. In the special case, $n = 5$, both the C33 and the C80 procedure coincide with the exact theory.

It is worth noticing critical rotation parameter values are taken from different investigations. While there is general consensus on the onset of barlike instabilities (in absence of tidal potential) at $v_c = 0.1871$ for $n = 0$ (e.g., Jeans 1929, Chap. VIII, §192), the contrary holds for the onset of equatorial breakup, as shown in Table 1. For $n = 1$, values from C80 were necessarily to be used in that values of $A_2(v)$ were also used in dealing with the C80 procedure. Related middle panels of Fig. 2 can be renormalized to the J64 (James 1964) value, $(v_c)_{J64} = 0.083720$, keeping in mind $0.8(v_c)_{C80} = 0.8 \times 0.10654 = 0.085232$, which implies the last upper two curves must be neglected for closer comparison with cases, $n = 1.5, 2, 3$. For $n = 4$, v_c has been taken from a different source (C85). A full list of values together with related references can be found in specific textbooks (e.g., Horedt 2004, Chap. 3, §3.8.8) with the addition of a few exceptions (e.g., C80) and recent attempts (e.g., Geroyannis and Karageorgopoulos 2014).

An inspection of Figs. 2 and 3 discloses the following.

- For small values of the rotation parameter, $v/v_c \approx 0.1-0.2$, the distortion indicator satisfies $\zeta_p \lesssim 0.1$ within the range of polytropic index, $0 \leq n < 5$, provided $\xi/\Xi_E \lesssim 0.8$.
- For large values of the rotation parameter, $v/v_c \approx 0.8-1.0$, the distortion indicator satisfies $\zeta_p \lesssim 0.1$ within the range, $0 \leq n \lesssim 1$, provided $\xi/\Xi_E \lesssim 0.4$; within the range, $1 \lesssim n \lesssim 2$, provided $\xi/\Xi_E \lesssim 0.5$; within the range, $2 \leq n < 5$, provided $\xi/\Xi_E \lesssim 0.6$.

Table 1: Values of rotation parameter at the onset of equatorial breakup, ν_R , for different values of polytropic index, n , taken from earlier investigations: James 1964 (J64), Hurley and Roberts 1964 (HR64), Monaghan and Roxburgh 1965 (MR65), Martin 1970 (M70), Naylor and Anand 1970 (NA70), C80, Horedt 1983 (H83), C85. The decimal notation after ν_R values, E- i , i natural number, is represented as $-i$ to save space.

n	ν_R							
	J64	HR64	MR65	M70	NA70	C80	H83	C85
0.0						0		6.6667-1
0.808	1.060296-1						1.22-1	1.3323-1
1.0	8.3720 -2		7.59-2			1.0654-1	9.46-2	1.2040-1
1.5	4.3624 -2	4.45-2	4.10-2	4.16-2	3.75-2		4.80-2	5.1942-2
2.0	2.1604 -2		1.99-2	2.14-2	1.94-2		2.34-2	2.4964-2
2.5	9.9300 -3	1.01-2	9.31-3	9.90-3			1.07-2	1.1513-2
3.0	3.932 -3	4.13-3	3.95-3	4.08-3	3.93-3		4.36-3	4.6946-3
3.5		1.40-3	1.25-3				1.48-3	1.5842-3
4.0		3.33-4	3.27-4	3.29-4	3.22-4		3.50-4	3.7434-4
4.75								3.9697-6
4.9				2.03-7	2.03-7		2.88-7	
5.0						0		0

- For all values of the rotation parameter, $0 \leq v/v_c \leq 1$, the distortion indicator satisfies $\zeta_p \lesssim 0.1$ in the special case, $n = 5$, within the range, $\xi/\Xi_E \leq 1$.

Let $\zeta_p \lesssim 0.1$ be assumed as a criterion for the validity, to an acceptable extent, of Eq. (13). According to the above results, it holds up to $\xi/\Xi_E \lesssim 0.8$ in the limit of low rotation parameter, $v/v_c \leq 0.1$, and roughly up to $\xi/\Xi_E \approx (n+8)/20$ in the limit of large rotation parameter, $0.9 \leq v/v_c \leq 1$, provided $n < 5$, while it holds up to $\xi/\Xi_E = 1$, regardless of the rotation parameter, provided $n = 5$. Outside the above mentioned ranges in ξ/Ξ_E , Eq. (13) no longer holds and the EC equation, Eq. (4a), should be integrated using a different kind of approximation, unless $n = 0, 1, 5$.

4 Dependence on n of selected parameters

The investigation of the dependence on the polytropic index, n , has been restricted to the following parameters: c_E/Ξ_E , d_0/Ξ_E , d_2/Ξ_E^3 , C_2 , $v_R \Xi_E^3$, which are related to well defined physical features, namely the continuity of the gravitational potential on the boundary and, concerning the last one, to the onset of equatorial breakup. As a first step, let the above mentioned functions be explicitly expressed in the special cases, $n = 0, 1, 5$.

With regard to the special case, $n = 0$, the substitution of Eqs. (58)-(61) into (52)-(54) after some algebra yields:

$$\frac{c_E}{\Xi_E} = 2 \quad ; \quad \frac{d_0}{\Xi_E} = 0 \quad ; \quad \frac{d_2}{\Xi_E^3} = 0 \quad ; \quad C_2 = -\frac{1}{6} \quad ; \quad n = 0 \quad ; \quad (101)$$

where the onset of equatorial breakup, $v_R = 0$, $\epsilon_R = 0$, as already mentioned, relates to an unstable configuration.

With regard to the special case, $n = 1$, the substitution of Eqs. (73)-(75) into (52)-(54) after some algebra yields:

$$\frac{c_E}{\Xi_E} = 1 \quad ; \quad \frac{d_0}{\Xi_E} = \frac{\pi^2}{3} - 1 \quad ; \quad \frac{d_2}{\Xi_E^3} = -\frac{15 - \pi^2}{3} \quad ; \quad C_2 = -\frac{\pi^2}{18} \quad ; \quad n = 1 \quad ; \quad (102)$$

where the value of rotation parameter at the onset of equatorial breakup, v_R , cannot be analytically expressed and depends on the method used, as shown in Table 1.

With regard to the special case, $n = 5$, the substitution of Eqs. (78)-(80) into (52)-(54) after some algebra yields:

$$\frac{c_E}{\Xi_E} = 0 \quad ; \quad \frac{d_0}{\Xi_E} = 0 \quad ; \quad \frac{d_2}{\Xi_E^3} = -\frac{1}{2} \quad ; \quad C_2 = -\frac{128}{45\pi} \quad ; \quad n = 5 \quad ; \quad (103)$$

where $\psi_0(\xi) \sim \xi^2/6$ as $\xi \rightarrow +\infty$ (H90) and the exact expression for finite ξ (H90) does not matter as $v \rightarrow 0$ in the case under consideration, $v\psi_0(\xi) \rightarrow 0$ for finite ξ , which makes the effect of distortion negligible therein (C87). At the onset of equatorial breakup, $\epsilon_R = 2/3$, $v_R \Xi_E^3 = 16\sqrt{3}/27$, via Eqs. (92)-(94).

The parameters under consideration are plotted as a function of the polytropic index, n , in Fig. 4, top left panel (c_E/Ξ_E , lower case; d_0/Ξ_E , upper case), top right panel (d_2/Ξ_E^3), bottom left panel (C_2), bottom right panel ($v_R \Xi_E^3$), where different symbols denote results from different sources, in particular squares (C85) and crosses (H90). Related interpolation curves are also shown together with analytical approximations in the neighbourhood of $n = 0, 5$, within the range, $0 \leq n \leq 0.5$, $5 \geq n \geq 4.5$, respectively. For a formal derivation and further details, an interested reader is addressed to Appendix B. The transition between instability towards bar modes (left) and equatorial breakup (right), $n = 0.808$, (James 1964), is marked by a dotted vertical line on the bottom right panel of Fig. 4.

With regard to an assigned empirical function, $f(n)$, and related fitting curve, $f_{\text{fit}}(n)$, the relative error may be expressed as:

$$R[f(n)] = 1 - \frac{f_{\text{fit}}(n)}{f(n)} ; \quad (104)$$

which is plotted in Fig. 5 for the cases of interest (from top to bottom), $f(n) = c_E/\Xi_E$, d_0/Ξ_E , d_2/Ξ_E^3 , C_2 , $v_R \Xi_E^3$, respectively, where different symbols denote results from different sources, in particular squares (C85) and crosses (H90).

An inspection of Figs. 4 and 5 discloses the following.

- The parameter, c_E/Ξ_E , matches to the limiting case, $n = 0$, for both C85 and H90 results. The parameters, d_0/Ξ_E , d_2/Ξ_E^3 , C_2 , $v_R \Xi_E^3$, match to the limiting case, $n = 0$, for C85 (d_0/Ξ_E unavailable) results, while the contrary holds for H90 ($v_R \Xi_E^3$ unavailable) results. The discrete domain is $n = \Delta n i$, where $\Delta n = 0.25$, $0 \leq i \leq 20$, with additional points in the neighbourhood of $n = 0, 5$, for C85 results and $\Delta n = 0.10$, $0 \leq i \leq 50$, for H90 results.
- The parameters, c_E/Ξ_E , C_2 , $v_R \Xi_E^3$, match to the limiting case, $n = 5$, for both C85 and H90 ($v_R \Xi_E^3$ unavailable) results, while the contrary holds with regard to the parameters, d_0/Ξ_E , d_2/Ξ_E^3 , for both C85 (d_0/Ξ_E unavailable) and H90 results.
- The parameter, $v_R \Xi_E^3$, exhibits a nonmonotonic trend in fission regime, $0 \leq n \leq 0.808$, for C85 results, even if the discrepancy with respect to numerical computations is unacceptably large.

- For $n \gtrsim 0$, $n \lesssim 5$, the analytical approximation provides an excellent fit to the results in connection with c_E/Ξ_E , no acceptable fit but a right trend in connection with C_2 , $v_R\Xi_E^3$, no acceptable fit and a worse trend (not shown) in connection with d_0/Ξ_E , d_2/Ξ_E^3 .
- The relative errors of the fitting curves lie within about 5% for both C85 and H90 results in connection with the parameters, c_E/Ξ_E , d_0/Ξ_E , d_2/Ξ_E^3 ($n \lesssim 4$), C_2 , and for results from numerical computations, (James 1964), in connection with the parameter, $v_R\Xi_E^3$. A larger discrepancy related to d_2/Ξ_E^3 ($n \gtrsim 4$), is due to increasingly smaller values as $n \rightarrow 5$ via Eq. (104).

5 Discussion

Open questions on the theory of EC polytropes have been focused as

- (1) What about the validity of EC associated equations, which imply the following approximations:

$$\begin{aligned}\theta^n &= [\theta_0 + A_2\theta_2P_2(\mu)]^n \approx \theta_0^n + n\theta_0^{n-1}A_2\theta_2P_2(\mu) \quad ; \\ \theta^n &= \{\theta_E + v[\psi_0 + C_2\psi_2P_2(\mu)]\}^n \approx \theta_E^n + vn\theta_E^{n-1}[\psi_0 + C_2\psi_2P_2(\mu)] \quad ;\end{aligned}$$

on a region sufficiently close to the boundary, where $\theta_0 \approx 0$ and $\theta_E \approx 0$?

- (2) What about the continuity of selected parameters as function of the polytropic index, n , in the close neighbourhood of the limiting cases, $n = 0, 5$?

Concerning (1), $\theta(\xi_0, \mu_0) = \theta_0(\xi_0)$ via Eqs. (16) and (19), within the framework of the extended EC approximation. Then the EC equation, Eq. (4a), for $\mu = \mu_0$ reduces to the EC associated equation of degree, $2\ell = 0$, Eq. (15), via Eqs. (12), (20), and the related solution holds all over the radially distorted sphere. On the other hand, Eq. (20) implies the validity of the EC associated equation of order, $2\ell = 2$, Eq. (15), provided μ is close enough to μ_0 . Then the related solution holds all over the radially distorted sphere. In fact, the EC associated functions, $\theta_{2\ell}$, depend only on the radial coordinate and remain unchanged along an arbitrary spherical surface centered on the origin.

This is why, though the validity of the EC associated equations appears restricted to a special region within the system, still their solutions hold at any point, provided θ_0^n is the real part of the principal value of the complex power within the range, $\Xi_0 < \xi < \Xi_e$, (Linnel 1981; C83; Geroyannis 1988;

Geroyannis and Karageorgopoulos 2014). More specifically, $\theta_{2\ell}$ must be conceived as the solutions of EC associated equations in the region where Eq. (13) holds to a good extent, and solutions of different versions of EC associated equations in the region where Eq. (13) is an unacceptable approximation.

The above results are valid for the EC associated functions, θ_0 and θ_2 , in the framework of the extended C33 approximation. The same holds for the EC associated functions, ψ_0 , ψ_2 , via Eqs. (47)-(49), in the framework of the C33 approximation.

Concerning (ii), among the selected parameters, the comparison between results from different sources (C85; H90) can be performed only for c_E/Ξ_E , d_2/Ξ_E^3 , C_2 . An inspection of Fig. 4 shows related results agree to a good extent for $n > 0.1$, while H90 results are lacking within the range, $0 < n < 0.1$. The sole significant discrepancy occurs for d_2/Ξ_E^3 at $n = 0.1$. The reason can be found in the parent papers, where the EC associated functions, ψ_0 , ψ_2 , and their first derivatives, match to their counterparts at $n = 0$ in one case (C85; ψ_0 unavailable), while the contrary holds in the other one (H90). The continuity is implied in that ψ_0 , ψ_2 , are related to the gravitational potential inside the body, which is expected to change continuously as the density profile tends to be flat.

To this respect, it is worth emphasizing the above mentioned attempts use different methods for solving the EC associated equations, namely series solutions (C85) and direct numerical integration (H90). The results are in perfect agreement with regard to the EC function and its first derivatives. The same holds for the EC associated function, $\theta_2(\Xi_E; v = 0) = \psi_2(\Xi_E)$ (ψ_0 has not been evaluated in C83) provided $n \geq 1$. On the contrary, significant discrepancies arise for $\theta_2(\Xi_E; v = 0) = \psi_2(\Xi_E)$, $\theta'_2(\Xi_E; v = 0) = \psi'_2(\Xi_E)$, for $n < 0.2$, $n < 0.5$, respectively, while $\theta''_2(\Xi_E; v = 0) = \psi''_2(\Xi_E)$ is divergent within the range, $0 < n < 0.5$, $0.5 < n < 1$, (C83). It can be seen no exact value of $\theta_{2\ell}(\Xi_E; v = 0) = \psi_{2\ell}(\Xi_E)$ can be obtained from numerical integration in the neighbourhood of $n = 0$ (H90). Accordingly, results inferred via series solutions must be preferred in this region, which ensures continuity (C83). Then the selected parameters may safely be thought of as continuous as the polytropic index, n , approaches 0 i.e. the system tends to be homogeneous.

In the opposite limit, $n \rightarrow 5$, the system tends to be infinitely extended or infinitely concentrated. The parameters, c_E/Ξ_E , C_2 , $v_R \Xi_E^3$, may safely be thought of as continuous, while the contrary holds for d_0/Ξ_E , d_2/Ξ_E^3 , where the trend remains monotonic as shown in Fig. 4. To this respect, two orders of considerations can be drawn. First, computations in the neighbourhood of $n = 5$ should be very accurate due to the divergence of Ξ_E , which maximizes the effect of the errors. Second, computations should be extended within the range, $4.9 < n < 5$, to recognize if the expected trend takes place.

6 Conclusion

With regard to polytropes, the isopycnic surfaces can be approximated as similar and similarly placed ellipsoids (exact for homogeneous configurations) for several investigations, such as the description of gravitational radiation from collapsing and rotating massive star cores, (Saens and Shapiro 1978, 1981), rigidly rotating and binary polytropes, (Lai et al. 1993, 1994a,b), gravitational collapse of nonbaryonic dark matter and related pancake formation, (Bisnovatyi-Kögan 2004, 2005).

In addition, inhomogeneous configurations sufficiently close to the extended Roche limit ($n \lesssim 5$) can be described, to an acceptable extent, in terms of properties related to extended Roche configurations ($n = 5$). A description of tenuous gas-dust atmospheres of some stars and tenuous haloes surrounding compact elliptical galaxies, in terms of extended Roche configurations, is mentioned in a recent investigation (Kondratyev and Trubitsina 2013).

On the other hand, numerical simulations have not been performed (to the knowledge of the author) outside the range, $0.1 \leq n \leq 4.9$. Then a first step in exploiting the limits, $n \rightarrow 0$, $n \rightarrow 5$, with regard to selected physical parameters, must necessarily be performed analytically.

The current attempt has been devoted to two specific points about EC polytropes, namely (i) the extent to which both C33 and extended C33 approximation are consistent with the binomial series approximation, $(\theta_w + \Delta\theta)^n \approx \theta_w^n + n\theta_w^{n-1}\Delta\theta$, keeping in mind $\theta_w \rightarrow 0$ on the boundary, $w = E, 0$, respectively, and (ii) the trend shown by selected parameters as a function of the polytropic index, n , in particular the continuity in the neighbourhood of the limiting cases, $n = 0, 5$. The main results may be summarized as follows.

- Though the validity of EC associated equations is restricted to a specific region within the system, still related solutions hold within the whole volume with regard to the EC associated functions, θ_0 , θ_2 , in the framework of the extended C33 approximation, and ψ_0 , ψ_2 , in the framework of the C33 approximation.
- The expected continuity of the parameters, c_E/Ξ_E , d_0/Ξ_E , d_2/Ξ_E^3 , C_2 , $v_R\Xi_E^3$, as a function of the polytropic index, n , has been safely verified as $n \rightarrow 0$ with the exception of d_0/Ξ_E , $v_R\Xi_E^3$, and as $n \rightarrow 5$ with the exception of d_0/Ξ_E , d_2/Ξ_E^3 , where additional data would be needed.
- Simple fits to the above mentioned functions are provided for a wide range of n , where the relative error does not exceed a few percent. Related curves are exponential depending on four parameters, with

the exception of C_2 , where two straight lines are joined by a parabolic segment.

The expression of physical parameters in terms of the polytropic index, n , can be used in building up sequences of configurations with changing density profile for assigned mass and angular momentum.

References

- [1] Binney, J., Tremaine, S., 1987. *Galactic Dynamics*, Princeton University Press, Princeton.
- [2] Caimmi, R., 1980. *Astrophys. Space Sci.* 71, 415. (C80).
- [3] Caimmi, R., 1983. *Astrophys. Space Sci.* 89, 255. (C83).
- [4] Caimmi, R., 1985. *Astrophys. Space Sci.* 113, 125. (C85).
- [5] Caimmi, R., 1987. *Astrophys. Space Sci.* 135, 347. (C87).
- [6] Caimmi, R., 1988. *Astrophys. Space Sci.* 140, 1. (C88).
- [7] Caimmi, R., 2006. *Serb. Astron. J.* 173, 13.
- [8] Chandrasekhar, S., 1933a. *Mon. Not. R. Astron. Soc.* 93, 390. (C33).
- [9] Chandrasekhar, S., 1933b. *Mon. Not. R. Astron. Soc.* 93, 539.
- [10] Chandrasekhar, S., 1939. *An introduction to the study of the stellar structure*, Dover Publications, Inc., University of Chicago Press.
- [11] Chandrasekhar, S., 1969. *Ellipsoidal Figures of Equilibrium*, Yale University Press, New Haven and London.
- [12] Chandrasekhar, S., Lebovitz, N.R., 1962. *Astrophys. J.* 136, 1082.
- [13] Dedekind, J.W.R., 1860. *J. Reine Angew. Math.* 58, pp. 217-228.
- [14] Emden, V.R., 1907. *Gaskugeln*, Verlag, B.G. Teubner, Leipzig, Berlin.
- [15] Geroyannis, V.S., 1988. *Astrophys. J.* 327, 273.
- [16] Geroyannis, V.S., Karageorgopoulos, V.G., 2014. *New Astron.* 28, 9.
- [17] Horedt, G.P., 1983. *Astrophys. J.* 269, 303.

- [18] Horedt, G.P., 1986. *Astrophys. Space Sci.* 126, 357.
- [19] Horedt, G.P., 1990. *Astrophys. J.* 357, 560. (H90).
- [20] Horedt, G.P., 2004. *Polytropes*, *Astrophys. Space Sci. Library* 306, Kluwer Academic Publishers, Dordrecht.
- [21] Hurley, M., Roberts, P.H., 1964. *Astrophys. J.* 140, 583.
- [22] Jacobi, C.G.J., 1834. *Poggendorff Annalen der Physik und Chemie* 33, 229-238, reprinted in *Gesammelte Werke* 2 (Berlin, G. Reimer, 1882), 17-72.
- [23] James, R.A., 1964. *Astrophys. J.* 140, 552.
- [24] Kondratyev, B.P., Trubitsina, N.G., 2013. *Astron. Nachr.* 334, 879.
- [25] Jeans, J., 1929. *Astronomy and Cosmogony*, Dover Publications, New York.
- [26] Lai, D., Rasio, F.A., Shapiro, S.L, 1993. *Astrophys. J. Supp.* 88, 205.
- [27] Lai, D., Rasio, F.A., Shapiro, S.L., 1994. *Astrophys. J.* 423, 344.
- [28] Lai, D., Rasio, F.A., Shapiro, S.L., 1994. *Astrophys. J.* 437, 742.
- [29] Lane, J.H., 1870. *Amer. J. Sci.*, 2nd ser., 1, 57-74.
- [30] Linnell, A.P., 1981. *Astrophys. Space Sci.* 76, 61.
- [31] MacLaurin, C., 1742. *A treatise on fluxions*.
- [32] MacMillan, W.D., 1930. *The theory of the potential*, Dover Publications, New York.
- [33] Martin, P.G., 1970. *Astrophys. Space Sci.* 7, 119.
- [34] Monaghan, F.F., Roxburgh, I.W., 1965. *Mon. Not. R. Astron. Soc.* 131, 13.
- [35] Naylor, M.D.T., Anand, S.P.S., 1970. *IAU Colloquium 4, Stellar Rotation*, ed. A. Slettebak (Dordrecht: Reidel), p.157.
- [36] Ritter, A., 1878. *Wiedemann Annalen* 6, 155.
- [37] Riemann, B., 1860. *Abh. d. Konigl. Gesew. der Wis. zu Gottingen* 9, pp.3-36.

- [38] Rodrigues, H., 2014. Mon. Not. R. Astron. Soc. 440, 1519.
- [39] Saenz, R.A., Shapiro, S.L., 1978. Astrophys. J. 221, 286.
- [40] Saenz, R.A., Shapiro, S.L., 1981. Astrophys. J. 244, 1033.
- [41] Schuster, A., 1883. Brit. Ass. Rept., p. 427.
- [42] Seidov, Z.F., Kuzakhmedov, R.Kh., 1978. Sov. Astron. 22, 711.
- [43] Thomson, W., 1887. Phil. Mag. 22, 287.
- [44] Vandervoort, P.O., 1980. Astrophys. J. 241, 316.
- [45] Vandervoort, P.O., Welty, D.E., 1981. Astrophys. J. 248, 504.

Appendix

A Slowly rotating isopycnic surfaces

In the limit of small rotation, $v \ll 1$, it may safely be thought the series, expressed by Eq. (16), reduces to:

$$\theta(\xi, \mu) = \theta_0(\xi) + A_2 \theta_2(\xi) P_2(\mu) = \kappa ; \quad (105)$$

$$P_2(\mu) = \frac{3}{2} \mu^2 - \frac{1}{2} ; \quad (106)$$

which implies $\theta(\xi_0, \mp \mu_0) = \theta_0(\xi_0)$, where $\mu_0 = \cos \delta_0 = 1/\sqrt{3}$, $\delta_0 = \arctan \sqrt{2}$. The dimensionless radius, $\xi_0 = \sqrt{[(\xi_0)_1]^2 + [(\xi_0)_3]^2}$, $(\xi_0)_1 = \xi_0 \sqrt{1 - \mu_0^2}$, $(\xi_0)_3 = \mp \xi_0 \mu_0$, may be geometrically determined in an elegant way, as shown in Fig. 6, along the following steps.

- Fix $(\xi_0)_3 = \xi_0 \mu_0$ and trace the square with side equal to $(\xi_0)_3$ and three vertexes on the non negative coordinate semiaxes.
- Trace the quarter of circle centered on the origin, with radius equal to the diagonal of the square defined above, lying on the first quadrant.
- Trace the square with side equal to the diagonal of the square defined above and three vertexes on the non negative coordinate semiaxes.
- Trace the continuation of the horizontal side of the former square defined above, parallel to the horizontal axis, up to the intersection with the vertical side of the latter square defined above, parallel to the vertical axis.

- The intersection defined above yields the point, $P_0 \equiv (\xi_0, +\mu_0) \equiv [(\xi_0)_1, (\xi_0)_3]$, and hence the locus, $(\xi_0, \mp\mu_0)$.

B Determination of fitting curves

With regard to the parameters of EC polytropes, plotted in Fig. 4, fitting curves shall be determined aiming to get simple expressions instead of best fits. To this end, a lot of symbols is needed, part of which has already been used throughout the text with a different meaning. The reader has to keep in mind that symbols denoting parameters of the fitting curves have no connection with their counterparts (if any) defined in the text.

In the neighbourhood of polytropic indexes where exact analytic results can be determined, $n = 0, 1, 5$, a series approximation can be developed (Seidov and Kuzackhmedov 1978; C88). Unfortunately, for $n = 0, 5$, the quantities of interest cannot be satisfactorily fitted, as shown by the broken lines (if any) plotted in Fig. 4. The sole exception is c_E/Ξ_E , where an excellent fit is provided within the range, $0 < n < 0.5$, $4 < n < 5$, as shown in Fig. 4, top left panel, lower case.

For $n \gtrsim 0$, the result is:

$$\frac{c_E}{\Xi_E} = 2[1 + (6 \ln 2 - 5)n] ; \quad (107)$$

$$\frac{d_0}{\Xi_E} = \left(8 \ln 2 - \frac{37}{3}\right) n ; \quad (108)$$

$$\frac{d_2}{\Xi_E^3} = 0 ; \quad (109)$$

$$C_2 = -\frac{1}{6} \left[1 + \frac{18}{25} \left(\frac{23}{15} - \ln 2\right) n\right] ; \quad (110)$$

$$v_R \Xi_E^3 = v_R(n) 6\sqrt{6} \left[1 + \left(6 \ln 2 - \frac{7}{2}\right) n\right] ; \quad (111)$$

$$\Xi_E = \sqrt{6} \left[1 + \left(2 \ln 2 - \frac{7}{6}\right) n\right] ; \quad (112)$$

where v_R is the value of the rotation parameter at the onset of equatorial breakup (leaving aside instabilities) for EC polytropes of index, n . In the limit, $n \rightarrow 0$, Eqs. (107)-(110) reduce to their exact counterparts, Eq. (101).

For $n \lesssim 5$, the result is:

$$\frac{c_E}{\Xi_E} = \frac{\pi}{32}(5 - n) ; \quad (113)$$

$$\frac{d_0}{\Xi_E} = 0 ; \quad (114)$$

$$\frac{d_2}{\Xi_E^3} = -\frac{1}{2} ; \quad (115)$$

$$C_2 = -\frac{128}{45\pi} ; \quad (116)$$

$$v_R \Xi_E^3 = v_R(n) \left(\frac{32\sqrt{3}}{\pi} \right)^3 \frac{1}{(5-n)^3} ; \quad (117)$$

$$\Xi_E = \sqrt{3} \left\{ \left[\frac{32}{\pi(5-n)} \right]^2 - 1 \right\}^{1/2} \approx \frac{32\sqrt{3}}{\pi(5-n)} ; \quad (118)$$

which coincide with or reduce to their exact counterparts, Eq. (103), as $n \rightarrow 5$.

For $n \approx 1$, a regular trend is shown by the data plotted in Fig. 4 and no analytical approximation is needed to gain further insight.

With regard to the parameter, C_2 , the fit has been performed in the following way. First, regression lines have been determined, using standard methods, close enough to and far enough from $n = 0$, respectively. The result is:

$$C_2 = a_U n + b_U ; \quad U = F, C ; \quad (119)$$

$$a_F = -2.10475 ; \quad b_F = -0.170428 ; \quad 0 \leq n \leq 0.1 ; \quad (120)$$

$$a_C = -0.0863467 ; \quad b_C = -0.464166 ; \quad 0.808 \leq n \leq 5 ; \quad (121)$$

as shown in Fig. 4, bottom left panel. The indexes, F, C, denote instability with respect to bar modes ($n < 0.808$) and equatorial breakup ($n \geq 0.808$), respectively. From this point on, in the case under discussion, the notation, $(OnC_2) = (Oxy)$, shall be used for simplicity.

Second, the straight lines are joined by a parabola requiring the following.

- The axis of the parabola coincides with the bisector of the angle formed by the regression lines, expressed as:

$$\gamma = \arctan \frac{a_C - a_F}{1 + a_C a_F} ; \quad (122)$$

according to standard results of analytic geometry.

- The first derivatives of the joining parabola, $p(x, y) = 0$, at the joining points, $P_F \equiv (x_F, y_F)$, $P_C \equiv (x_C, y_C)$, equal the slope of related regression lines, as:

$$\left(\frac{\partial p}{\partial x} \right)_{P_U} = a_U ; \quad U = F, C ; \quad (123)$$

or, in other words, the joining parabola is tangent to the regression lines at the points, P_F , P_C , respectively.

For determining the equation of the parabola, a change of reference frame is needed, where the new origin, Q , coincides with the intersection point between the regression lines, $P_I \equiv (x_I, y_I)$, the vertical axis, Y , coincides with the bisector of the angle, γ , formed by the regression lines, and the chirality is preserved i.e. (Oxy) and (QXY) can be superimposed on the common plane.

The explicit expression of the coordinates of the intersection point reads:

$$x_I = -\frac{b_F - b_C}{a_F - a_C} ; \quad y_I = \frac{a_F b_C - a_C b_F}{a_F - a_C} ; \quad (124)$$

according to standard results of analytic geometry.

Finally, the change of reference frame takes the expression:

$$\begin{cases} X = (x - x_I) \cos \theta - (y - y_I) \sin \theta ; \\ Y = (x - x_I) \sin \theta + (y - y_I) \cos \theta ; \end{cases} \quad (125)$$

where θ is the angle between the starting axis, y , and the resulting axis, Y , i.e. the bisector of the angle, γ .

The related explicit expression reads:

$$\theta = -\frac{1}{2}(\arctan a_F + \arctan a_C) ; \quad (126)$$

according to standard results of analytic geometry.

With regard to the resulting reference frame, (QXY) , the regression lines intersect at the origin, $Q \equiv P_I$, and exhibit equal and opposite slopes as:

$$a' = -a'_F = a'_C = -\tan \frac{\gamma}{2} = \tan \left(\frac{1}{2} \arctan \frac{a_C - a_F}{1 + a_C a_F} \right) ; \quad (127)$$

according to standard results of analytic geometry.

In addition, the joining points, $P_F \equiv (X_F, Y_F)$, $P_C \equiv (X_C, Y_C)$, are symmetrical with respect to the Y axis as:

$$-X_F = X_C ; \quad Y_F = Y_C ; \quad (128)$$

and the equation of the parabola reduces to:

$$Y = P(X) = AX^2 + C ; \quad (129)$$

where the term in X is ruled out by the above mentioned symmetry.

For assigned (x_F, y_F) or (x_C, y_C) , (X_F, Y_F) and (X_C, Y_C) can be determined via Eqs. (124)-(128). The remaining point, (x_C, y_C) or (x_F, y_F) , can be determined inverting Eq. (125) as:

$$\begin{cases} x = x_I + X \cos \theta + Y \sin \theta ; \\ y = y_I - X \sin \theta + Y \cos \theta ; \end{cases} \quad (130)$$

and particularizing to $(x, y) = (x_C, y_C)$ or $(x, y) = (x_F, y_F)$; $(X, Y) = (X_C, Y_C)$ or $(X, Y) = (X_F, Y_F)$; respectively.

The coefficients, A, C , appearing in Eq. (129), can be expressed keeping in mind the joining parabola is tangent to the regression lines at (X_F, Y_F) and (X_C, Y_C) . The result is:

$$A = -\frac{1}{2} \frac{a'}{X_F} = \frac{1}{2} \frac{a'}{X_C} ; \quad (131)$$

$$C = Y_F + \frac{1}{2} \frac{a'}{X_F} = Y_C - \frac{1}{2} \frac{a'}{X_C} ; \quad (132)$$

and the equation of the parabola in the starting reference frame, $p(x, y) = 0$, can be determined inserting Eqs. (125), (131), (132), into (129).

In summary, the above mentioned procedure acts along the following steps.

- (a) Choose a joining point, $P_U \equiv (x_U, y_U)$, on the regression line, $y = a_U x + b_U$, $U = F$ or $U = C$.
- (b) Change the reference frame from (Oxy) to (QXY) .
- (c) With regard to the resulting frame, (QXY) , determine the joining points, $P_F \equiv (X_F, Y_F)$, $P_C \equiv (X_C, Y_C)$, where $-X_F = X_C$, $Y_F = Y_C$.
- (d) With regard to the starting frame, (Oxy) , determine the joining point, $P_V \equiv (x_V, y_V)$, $V = C$ or $V = F$.
- (e) With regard to the resulting frame, (QXY) , determine the coefficients in the expression of the parabola, Eq. (129).
- (d) With regard to the starting frame, (Oxy) , write the explicit expression of the equation of the parabola, $p(x, y) = 0$.

The parameters of the joining parabola are found to be:

$$(x_F, y_F) = (0.1, 0.380903) ; \quad (x_C, y_C) = (0.251231, 0.485859) ; \quad (133)$$

$$A = 3.11439 ; \quad C = 0.026384 ; \quad (134)$$

and the related fitting curve can be determined by use of Eqs. (119), (120), (121), (133), (134), and plotted in Fig. 4, bottom left panel. The relative error, $R(C_2)$, is shown in Fig. 5, intermediate bottom panel.

With regard to the remaining parameters, c_E/Ξ_E , d_0/Ξ_E , d_2/Ξ_E^3 , $\nu_R\Xi_E^3$, a fitting exponential function has been chosen, as:

$$y = f(x) = C_1 \exp(-C_2 x^\gamma) + C_3 \quad ; \quad (135)$$

where $x = n$, $y = f(x)$ is the parameter of interest, and C_1 , C_2 , C_3 , γ , are constants to be determined. The related boundary conditions are:

$$f(0) = C_1 + C_3 = y_0 \quad ; \quad (136)$$

$$f(1) = C_1 \exp(-C_2) + C_3 = y_1 \quad ; \quad (137)$$

$$f(2) = C_1 \exp(-C_2 2^\gamma) + C_3 = y_2 \quad ; \quad (138)$$

$$f(5) = C_1 \exp(-C_2 5^\gamma) + C_3 = y_5 \quad ; \quad (139)$$

where y_0 , y_1 , y_5 , can be analytically expressed and y_2 has to be numerically computed.

The substitution of Eq. (136) into (135) after some algebra yields:

$$\exp(-C_2) = \left(\frac{C_1 - y_0 + y}{C_1} \right)^{1/x^\gamma} \quad ; \quad \frac{C_1 - y_0 + y}{C_1} > 0 \quad ; \quad (140)$$

where the inequality must necessarily hold owing to (i) the exponential function is always positive and (ii) the real basis of a power with a real exponent is defined for non negative values.

Let (x_A, y_A) , (x_B, y_B) , (x_C, y_C) , be generic points for which the coordinates are known. The particularization of Eq. (140) to (x_A, y_A) , (x_B, y_B) , and the combination of related expressions, after some algebra yields:

$$\gamma \ln \frac{x_B}{x_A} = \ln \ln \frac{C_1 - y_0 + y_B}{C_1} - \ln \ln \frac{C_1 - y_0 + y_A}{C_1} \quad ; \quad (141)$$

and the combination of Eq. (141) with its counterpart related to (x_A, y_A) , (x_C, y_C) , after some algebra produces:

$$\begin{aligned} & \ln \frac{x_C}{x_A} \left[\ln \ln \frac{C_1 - y_0 + y_B}{C_1} - \ln \ln \frac{C_1 - y_0 + y_A}{C_1} \right] \\ &= \ln \frac{x_B}{x_A} \left[\ln \ln \frac{C_1 - y_0 + y_C}{C_1} - \ln \ln \frac{C_1 - y_0 + y_A}{C_1} \right] \quad ; \quad (142) \end{aligned}$$

where the intersection of related curves yields the value of C_1 .

In the case under discussion, $(x_A, y_A) = (1, y_1)$, $(x_B, y_B) = (2, y_2)$, $(x_C, y_C) = (5, y_5)$, and Eq. (142) reduces to:

$$\begin{aligned} & \ln 5 \left[\ln \ln \frac{C_1 - y_0 + y_2}{C_1} - \ln \ln \frac{C_1 - y_0 + y_1}{C_1} \right] \\ &= \ln 2 \left[\ln \ln \frac{C_1 - y_0 + y_5}{C_1} - \ln \ln \frac{C_1 - y_0 + y_1}{C_1} \right] ; \end{aligned} \quad (143)$$

where the knowledge of C_1 together with y_0, y_1, y_2, y_5 , makes the remaining parameters, C_2, C_3, γ , be inferred from Eqs. (136)-(139). Related fitting curves are shown in Fig. 4, top left, top right and bottom right panels. For further details, each case must be discussed separately.

With regard to the function, $f(n) = c_E/\Xi_E$, plotted in Fig. 4, top left panel, lower case, the parameters of the fitting curve are found to be:

$$C_1 = 2.28169 ; C_2 = 0.576739 ; C_3 = -0.281685 ; \gamma = 0.800546 ; \quad (144)$$

related to the input parameters:

$$y_0 = 2 ; y_1 = 1 ; y_2 = 0.553897 ; y_5 = 0 ; \quad (145)$$

and the relative error, $R[f(n)]$, is shown in Fig. 5, extreme top panel.

With regard to the function, $f(n) = d_0/\Xi_E$, plotted in Fig. 4, top left panel, upper case, the parameters of the fitting curve are found to be:

$$C_1 = 1.57191 ; C_2 = 0.601048 ; C_3 = 1.42809 ; \gamma = 0.809883 ; \quad (146)$$

related to the input parameters:

$$y_0 = 3 ; y_1 = \frac{\pi^2}{3} - 1 \approx 2.29987 ; y_2 = 1.97614 ; y_5 = 1.6 ; \quad (147)$$

and the relative error, $R[f(n)]$, is shown in Fig. 5, intermediate top panel.

With regard to the function, $f(n) = d_2/\Xi_E^3$, plotted in Fig. 4, top right panel, the parameters of the fitting curve are found to be:

$$C_1 = -1.63794 ; C_2 = 0.500459 ; C_3 = 0.137937 ; \gamma = 0.993033 ; \quad (148)$$

related to the input parameters:

$$y_0 = -1.5 ; y_1 = -\frac{15 - \pi^2}{6} \approx -0.855066 ; y_2 = -0.466983 ; y_5 = 0 ; \quad (149)$$

and the relative error, $R[f(n)]$, is shown in Fig. 5, middle panel.

With regard to the function, $f(n) = v_R \Xi_E^3$, plotted in Fig. 4, bottom right panel, the parameters of the fitting curve are found to be:

$$C_1 = 3.07748 ; C_2 = 0.609298 ; C_3 = 0.922519 ; \gamma = 1.06613 ; \quad (150)$$

related to the input parameters:

$$y_0 = 4 ; y_1 = 2.59585 ; y_2 = 1.78182 ; y_5 = \frac{16\sqrt{3}}{27} \approx 1.02640 ; \quad (151)$$

and the relative error, $R[f(n)]$, is shown in Fig. 5, extreme bottom panel.

In addition, the combination of Eqs. (118), (135), (150), yields:

$$v_R = \left[\frac{\pi(5-n)}{32\sqrt{3}} \right]^3 [C_1 \exp(-C_2 n^\gamma) + C_3] ; \quad (152)$$

which is expected to hold to a good extent within the range, $4 \leq n \leq 5$, avoiding computational errors due to large values of the dimensionless radius, Ξ_E .

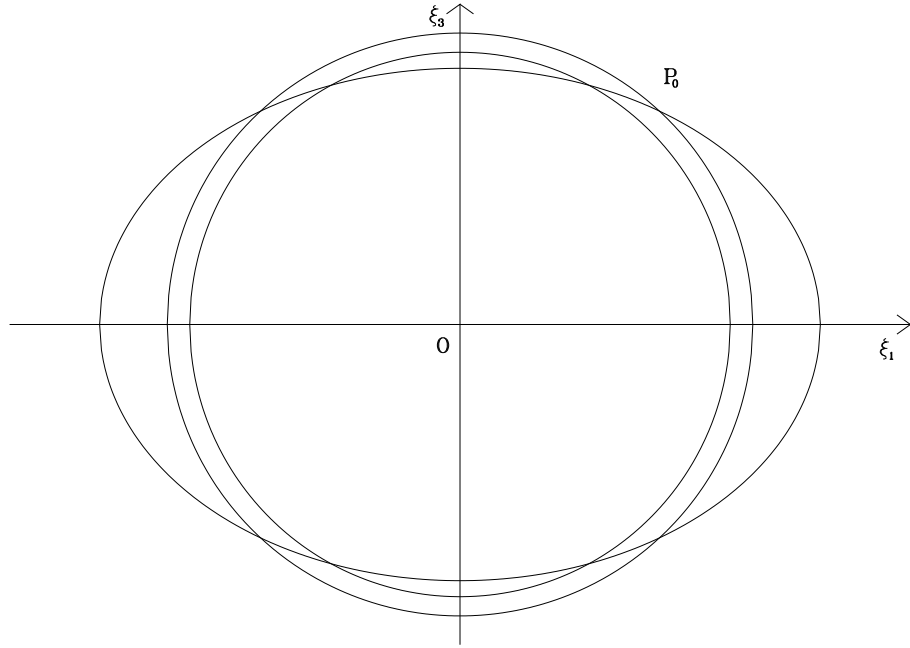


Figure 1: Generic isopycnic surfaces related to an assigned polytrope in the nonrotating limit (inner spherical), $\theta_E(\xi_E) = \kappa$, and in rigid rotation (oblate), $\theta(\xi, \mu) = \kappa$. The (fictitious) isopycnic surface of the expanded sphere (outer spherical), $\theta_0(\xi_0) = \kappa$, is also shown. Outer spherical and oblate isopycnic surfaces intersect at the locus, $(\xi_0, \mp\mu_0)$, where $\mu_0 = \cos \delta_0$, δ polar angle, e.g., $P_0 \equiv [|(\xi_0)_1|, |(\xi_0)_3|]$, $(\xi_0)_1 = \xi_0 \sqrt{1 - \mu_0^2}$, $(\xi_0)_3 = \mp \xi_0 \mu_0$. For further details refer to the text.

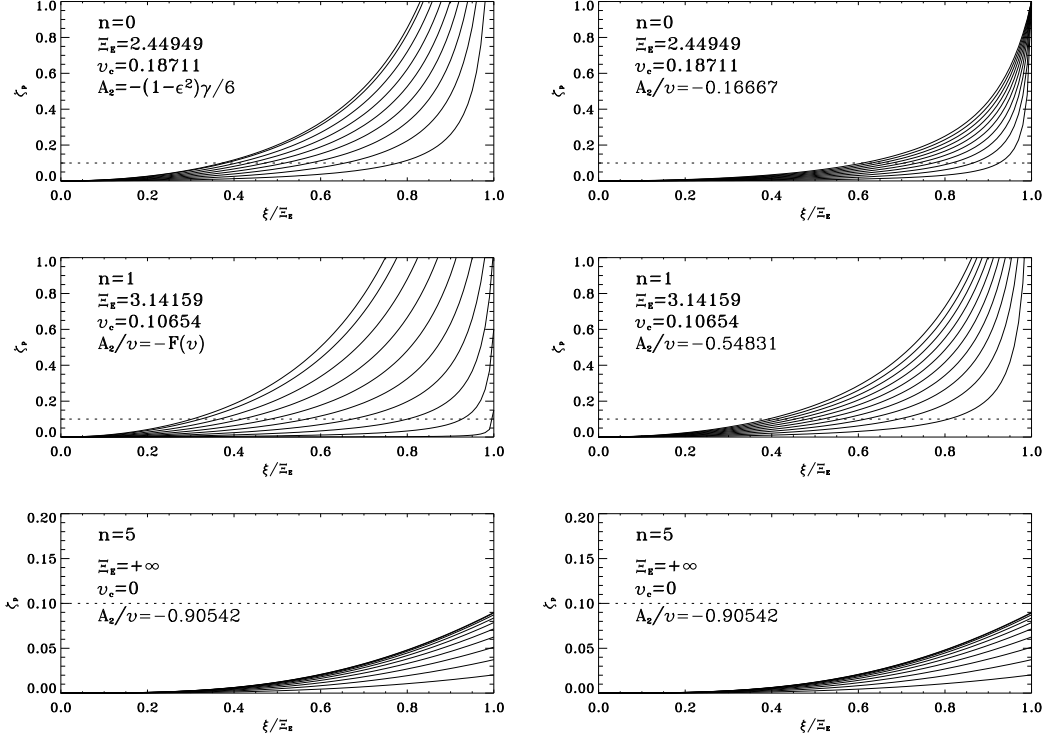


Figure 2: The distortion indicator, ζ_p , against the fractional dimensionless radial coordinate, ξ/Ξ_E , for polytropic index values, $n = 0, 1, 5$. Different curves relate to different rotation parameter values, $v/v_c = 0.1, 0.2, \dots, 1.0$, from bottom to top, where v_c is a critical value denoting the onset of instability against bar modes ($n \lesssim 0.808$) or equatorial breakup ($n \gtrsim 0.808$). Left and right panels relate to the C80 and C33 procedure, respectively, which are coincident in the special case, $n = 5$, where the vertical scale is enlarged. For further details refer to the text.

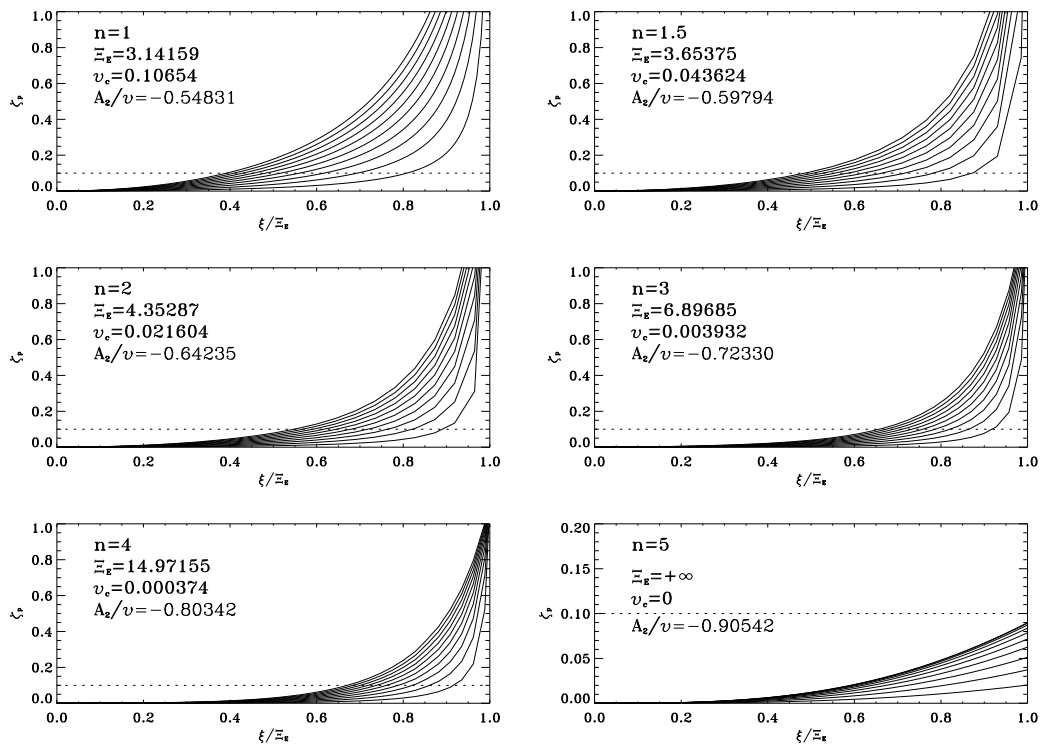


Figure 3: As in Fig. 2 but for $n = 1.5, 2, 3, 4$, according to the C33 procedure. Additional cases already plotted in Fig. 2, $n = 1, 5$, are added for better comparison.

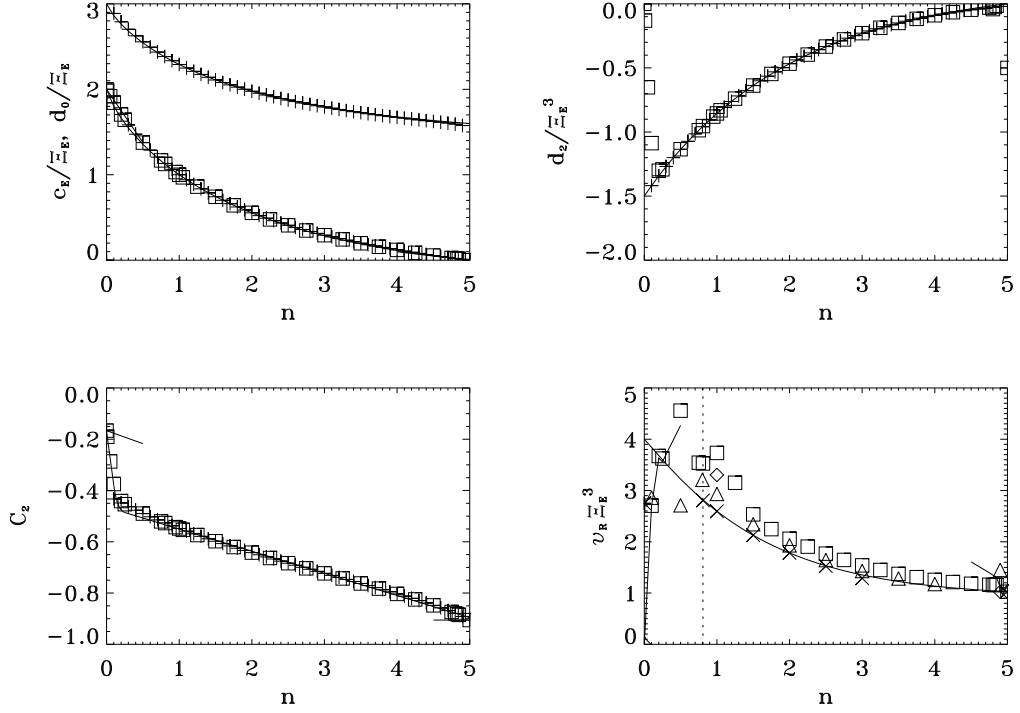


Figure 4: Parameters of rigidly rotating polytropes, c_E/Ξ_E (squares), d_0/Ξ_E (crosses), top left, d_2/Ξ_E^3 , top right, C_2 , bottom left, $v_R \Xi_E^3$, bottom right, as a function of the polytropic index, n . Source of results: squares (C85); crosses (H90); triangles (Horedt 1983); saltires (James 1964); diamonds C80 or quoted therein or quoted elsewhere (Horedt 2004); asterisks (Jeans 1929). Curves represent simple fits to the data. Series approximation are shown as broken lines. The vertical dotted line on the bottom right panel marks the boundary between instability towards bar modes (left) and equatorial breakup (right). See text for further details

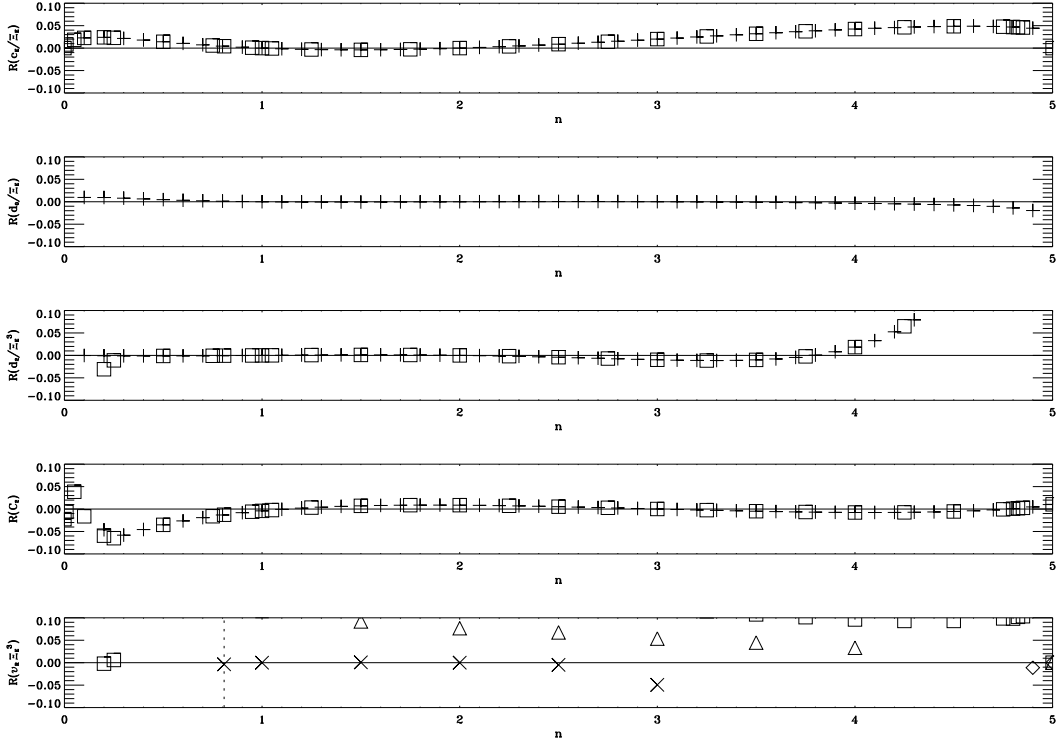


Figure 5: The relative error, $R[f(n)] = 1 - f_{\text{fit}}(n)/f(n)$, as a function of the polytropic index, n , for (from top to bottom) $f(n) = c_E/\Xi_E$, d_0/Ξ_E , d_2/Ξ_E^3 , C_2 , $v_R \Xi_E^3$, where f_{fit} relates to the fitting curve and f to results from different sources plotted with the same symbols as in Fig. 4.

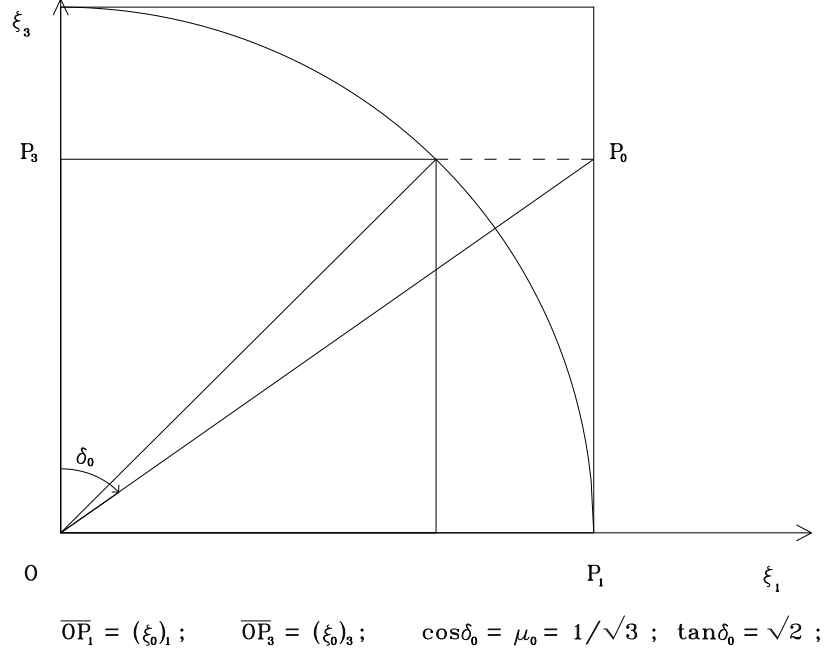


Figure 6: Determination of the intersection point, $P_0 \equiv (\xi_0, +\mu_0) \equiv [(\xi_0)_1, (\xi_0)_3]$, $(\xi_0)_1 = \xi_0\sqrt{1 - \mu_0^2}$, $(\xi_0)_3 = \xi_0\mu_0$, between fictitious (spherical) isopycnic surfaces, $\theta_0(\xi_0) = \kappa$, and rigidly rotating (oblate) isopycnic surfaces, $\theta(\xi, \mu) = \kappa$, and hence the locus of intersection points, $(\xi_0, \mp\mu_0)$, in the limit of small rotation. (i) Fix $(\xi_0)_3$ and trace the square with side equal to $(\xi_0)_3$ and three vertexes on the non negative coordinate semiaxes. (ii) Trace the quarter of circle centered on the origin, with radius equal to the diagonal of the square defined in (i), lying on the first quadrant. (iii) Trace the square with side equal to the diagonal of the square defined in (i) and three vertexes on the non negative coordinate semiaxes. (iv) Trace the continuation of the horizontal side of the square defined in (i), parallel to the horizontal axis, up to the intersection with the vertical side of the square defined in (iii), parallel to the vertical axis. (v) The intersection defined in (iv) yields the point, $P_0 \equiv (\xi_0, +\mu_0) \equiv [(\xi_0)_1, (\xi_0)_3]$, and hence the locus, $(\xi_0, \mp\mu_0)$.